Review Article

Structural Snapshots of Human tRNA Modifying Enzymes ☆

Alexander Hammermeister [1,*,†], Monika Gaik [1,†], Priyanka Dahate [1,2,†], and Sebastian Glatt [1,3,*]

*1 - **Malopolska Centre of Biotechnology (MCB),** Jagiellonian University, Krakow, Poland*
*2 - **Doctoral School of Exact and Natural Sciences,** Jagiellonian University, Krakow, Poland*
*3 - **Department for Biological Sciences and Pathobiology,** University of Veterinary Medicine Vienna, Vienna, Austria*

Correspondence to Alexander Hammermeister and Sebastian Glatt: Malopolska Centre of Biotechnology (MCB), Jagiellonian University, Krakow, Poland. *alexander.hammermeister@uj.edu.pl (A. Hammermeister), sebastian.glatt@uj.edu.pl (S. Glatt)*
https://doi.org/10.1016/j.jmb.2025.169106
Edited by Ute Kothe

Abstract

Cells use a plethora of specialized enzymes to post-transcriptionally introduce chemical modifications into transfer RNA (tRNA) molecules. These modifications contribute novel chemical properties to the affected nucleotides and are crucial for the tRNA maturation process and for most other aspects of tRNA biology. Whereas, some of the modifications are ubiquitous and the respective modifying enzymes are conserved in all domains of life, other modifications are found only in specific organisms, in specific tRNAs or at specific positions of tRNAs. Despite the fact, that evolution has shaped a tremendous variety of tRNA modifications and the respective modification cascades, the clinical relevance of patient-derived mutations has recently led to an increased interest in the set of human tRNA modifying enzymes. Over decades macromolecular crystallography has immensely contributed to understand the enzymatic function of tRNA modifying enzymes at the molecular level. The advent of high resolution single-particle cryo-EM has recently led to structures of several clinically relevant human tRNA modifying enzymes in complex with tRNAs and a more fundamental understanding of the mechanistic consequences of specific disease-related mutations. Here, we aim to provide a comprehensive summary of the currently available experimentally determined structures of human tRNA modifying enzymes.

Introduction

Ribonucleic acid (RNA) molecules are built up by four standard nucleotides, namely adenine (A), cytosine (C), guanine (G), and uracil (U) that are linked with a pentose sugar and phosphate groups. However, the post-transcriptional incorporation of chemical modifications greatly expands the diversity of the available RNA building blocks.[1,2] The incorporation of chemical groups contributes additional biophysical properties to the individual RNA bases and affects the folding, stability and formation of secondary structures in RNAs.[3,4] The regularly updated "Modomics" database for RNA modification[5,6] currently lists ~330 unique modified RNA nucleosides (including intermediates) that naturally occur in all domains of life. The database has been updated regularly since

☆ This article is part of a special issue entitled: 'tRNA modifications (2025)' published in Journal of Molecular Biology.

2006 and more than 100 unique RNA modifications can be found in tRNAs.[7]

These short noncoding RNAs are responsible for translating genomic information into functional polypeptides, also known as proteins or enzymes.[8] tRNA can vary in their sequences, but basically all functional tRNAs need to fold into the same three-dimensional structure,[9,10] which is conserved among almost all organisms.[11] On average, each tRNA molecule carries approximately 13 modified nucleotides[5] and the anticodon stem loop (ASL) region represents a "modification hotspot".[12] The recent advent of several high-throughput methods allows the quantitative assessment of intracellular tRNA levels and the detection of individual tRNA modifications.[13–18] Most modifications in the core regions of tRNAs affect their folding and stability,[19–21] whereas modification around the anticodon influence the dynamics of translational decoding[22–27] and subsequently affect co-translational folding dynamics,[28,29] proteome stability and cell survival.[30,31]

Interestingly, the expansion of tRNA gene copy numbers and *iso*-acceptors are evolutionary traits that separate the main kingdoms of life. These trends also correlate well with an increase in different tRNA modification enzymes, suggesting ongoing co-evolutionary mechanisms, which expand the decoding potential of the available tRNA pool and constantly optimize translational efficiency and accuracy via different tRNA modification pathways.[32] The majority of enzymatic cascades responsible for the human tRNA modification have been identified and confirmed in the last two decades.[33] Of note, all tRNAs have a similar domain architecture, folding pattern, molecular mass and charge distribution.[34] This high similarity between all cellular tRNA molecules represents a challenge for tRNA-binding proteins to achieve specificity and to find the correct set of target tRNAs. Hence, modifying enzymes do not only need to evolve around the active site to provide the correct chemical environment for catalysis, but they also need to evolve to correctly recognize and position tRNAs during the individual steps of the modification reactions.[34]

Clinically-relevant mutations in cytoplasmic tRNA genes are rare,[35] but an increasing number of patient-derived mutations has been identified in genes coding for tRNA modifying enzymes. The direct connection between tRNA biogenesis, human health and the onset of severe diseases has been summarized in several excellent reviews.[33,36–38] To identify disease-relevant genomic variants and to understand the mechanistic consequences of patient-derived mutations, it is beneficial to structurally and biochemically characterize human tRNA modifying enzymes and to reconstitute their modification cascades/reactions *in vitro*.

Here we aim to summarize currently available data of how to produce and purify the majority of individual human tRNA modification enzymes and complexes. We focus on those human tRNA modifying enzymes for which experimentally derived structural information has been publicly deposited. However, we discuss the possibility of using structures of homologues and *de novo* structure predictions to get useful structural insights for those human modifiers for which no experimentally determined structures are available. The provided inventory should encourage experts to access available structural data and to use spatial information to discover new tRNA biology. Foremost, this review represents a complementary resource for clinical researchers that would like to directly locate the position of patient-derived variants and to derive a structure–activity-relationship for those variants in human tRNA modifying enzymes.

Available structures of individual human tRNA modifying enzymes

In this section, we highlight the available structures of individual human tRNA modifying enzymes obtained in the absence of substrate tRNAs (Figure 1 and Table 1).

Dihydrouridine synthase 2 (DUS2)

Human DUS2 is involved in the reduction of U_{20} to form dihydrouridine (D_{20}) in multiple human tRNAs. The crystal structures of the catalytic and tRNA-binding domains have been solved separately. Both protein constructs have been cloned into the pEFX-04 vector and expressed in *Escherichia coli* (*E. coli*) BL21 (DE3) Star Codon Plus cells. The catalytic construct (residues 1–340) has been purified by immobilized metal affinity chromatography (IMAC) and size exclusion chromatography. The crystal structure was solved at a resolution of 1.9 Å and shows the catalytic TIM-barrel, the 5-helix bundle, the 3-stranded β-sheet insertion, and a flavin mononucleotide (FMN) cofactor bound in the active site in proximity of the catalytic cysteine residue (Cys116) (PDB ID 4XP7, Figure 1A).[39] The separately produced double stranded RNA binding domain (dsRBD) fragment (residues Δ347–451) also binds tRNAs by itself.[40] The expressed human protein is monomeric (~37 kDa) and has been shown to be active in dihydrouridylation assays *in vitro*.[41] High levels of human DUS2 have been linked to non-small cell lung cancer (NSCLC),

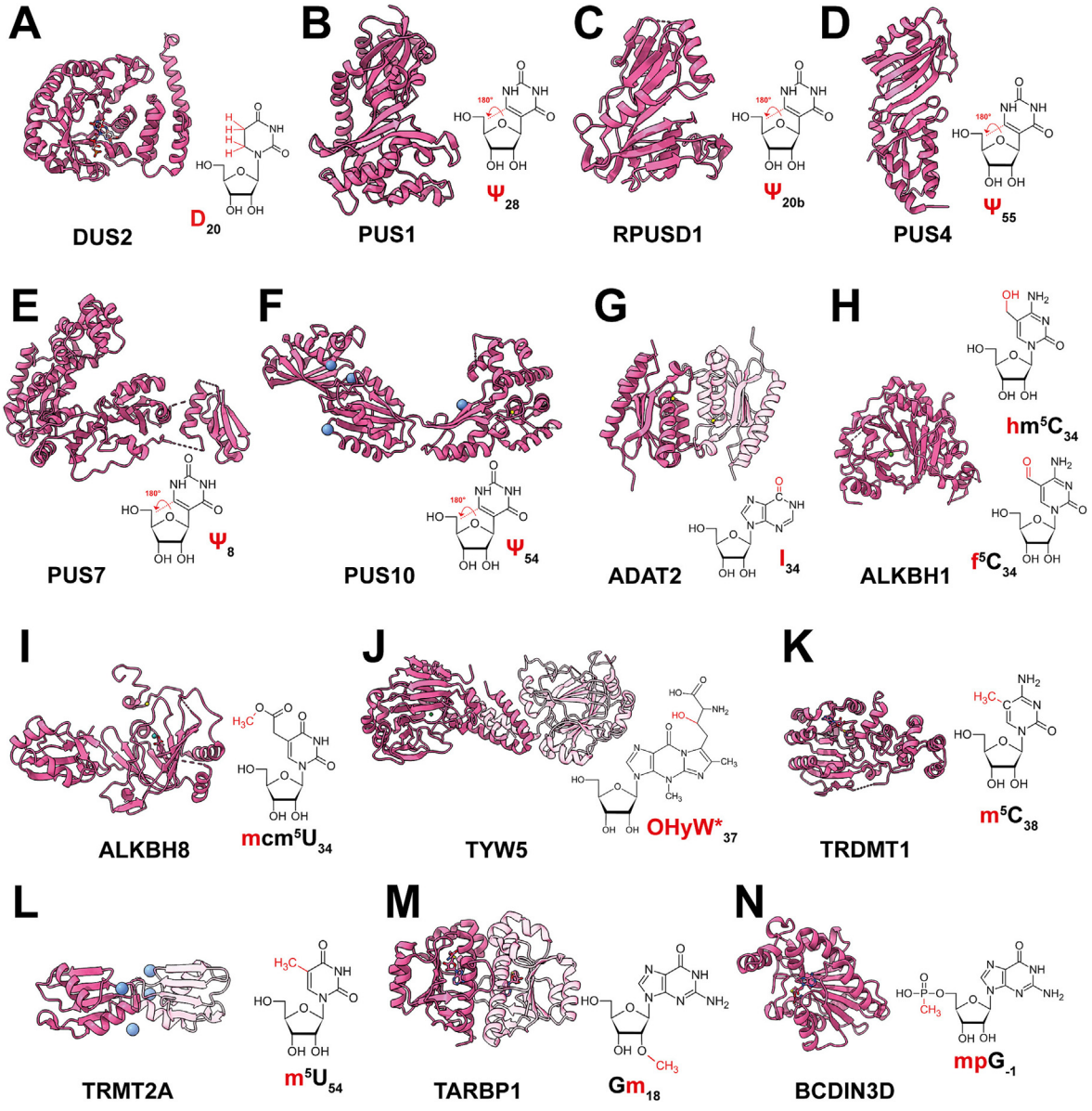

Figure 1. A gallery of structures of the individual human tRNA modification enzymes. Structural models determined by X-ray crystallography are shown in cartoon representation. Next to each model representative examples of chemical modifications introduced into nucleobases are displayed and the modifications are marked in red. The bound ions are depicted in blue (Cl^-) for PUS10 and TRMT2A, yellow (Zn^{2+}) for PUS10, ADAT2 and ALKBH8, green (Mg^{2+}) for TYW5, light green (Mn^{2+}) for ALKBH1 and ALKBH8. The other subunits of homodimers are colored in light pink (ADAT2, TYW5, TRMT2A, TARBP1). (A) DUS2 (PDB ID 4XP7), (B) PUS1 (PDB ID 4IQM), (C) RPUSD1 (PDB ID 5VBB), (D) PUS4 (PDB ID 8JFX), (E) PUS7 (PDB ID 5KKP), (F) PUS10 (PDB ID 2V9K), (G) ADAT2 (PDB ID 3DH1), (H) ALKBH1 (PDB ID 6 IE3), (I) ALKBH8 (PDB ID 3THP), (J) TYW5 (PDB ID 3AL5), (K) TRDMT1 (PDB ID 1G55), (L) TRMT2A (PDB ID 7NTO), (M) TARBP1 (PDB ID 2HA8), (N) BCDIN3D (PDB ID 6L8U).

contributing to worse disease progression and prognosis.[42]

Pseudouridine Synthase 1 (PUS1)

Human PUS1 converts specific uridine residues into pseudouridine (Ψ) in several non-coding RNAs, including tRNAs (at U_{26}, U_{27}, U_{28}, U_{30}, U_{34}, or U_{67}), as well as U2 spliceosomal RNA and steroid receptor activator RNA. Pseudouridylation, which does not require any cofactors, increases stability of the tertiary structure of RNA to ensure the accurate and efficient translation.[43] The genetic construct expressing residues 79–408 of PUS1 has been cloned into the pET47 vector and expressed in the BL21 (DE3) strain of *E. coli*. The recombinant protein was purified by IMAC, human Rhinovirus (HRV) 3C protease cleavage and size exclusion

Table 1 Summary of available structures of human tRNA modifying enzymes.

Enzyme Name	tRNA modification site	Modification	Structure determination technique	PDB IDs	Highest available resolution [Å]	Expression host	Construct
DUS2	U_{20}	D	X-ray	**4XP7**, 4WFS	1.9	*E. coli* BL21 (DE3) Star Codon Plus	1–340
PUS1	U_{26}, U_{27}, U_{28}, U_{30}, U_{34}, U_{67}	Ψ	X-ray	**4IQM**, 4ITS, 4J37	1.8	*E. coli* BL21(DE3)	79–408
RPUSD1	U_{20b}, U_{31}, U_{32}, $e_{11\text{-}14}$, U_{50}, U_{72}	Ψ	X-ray	5VBB	1.9	*E. coli*	1–261
PUS4	U_{55}	Ψ	X-ray	8JFX	2.2	*E. coli* Rosetta (DE3)	58–318
PUS7	U_8, U_{13}, U_{35}	Ψ	X-ray	5KKP	2.3	*E. coli* BL21(DE3)-V3R-pRARE2	99–661
PUS10	U_{54}, U_{55}	Ψ	X-ray	2V9K	2.0	*S. frugiperda* Sf-9	1–529 Δ63–75
ADAT2	A_{34}	I	X-ray	3DH1	2.8	*E. coli*BL21 (DE3)	1–191
ALKBH1	m^5C_{34}	hm^5C, f^5C	X-ray	6 IE3	2.0	*E. coli* BL21(DE3)	1–389
ALKBH8	cm^5U_{34}	mcm^5C	X-ray	3THP	3.2	*E. coli* B834(DE3)	25–354
TYW5	$yW\text{-}72_{37}$	OHyW-72	X-ray	3AL5	2.5	*E. coli* C41(DE3)	1–311
TRDMT1	C_{38}	m^5C	X-ray	1G55	1.8	*E. coli* McrBC-deficient strain ER2488	1-391 Δ191–237
TRMT2A	U_{54}	m^5U	X-ray	**7NTO**, 7NTN	1.2	*E. coli* Rosetta	69–147
TARBP1	G_{18}	G_m	X-ray	2HA8	1.6	*E. coli* BL21 (DE3) Codon Plus RIL	1438–1621
BCDIN3D	G_{-1}	mpG	X-ray	6L8U	2.9	*E. coli* BL21 (DE3)	14–284 Δ92–99
TGT (QTRT1/2) complex	G_{34}	Q	cryo-EM	8OMR	3.3	*E. coli* BL21 (DE3)	Full-length
PUS3	U_{38}, U_{39}	Ψ	cryo-EM	9F9Q, 8OKD, **9ENB**, 9ENC, 9ENE, 9ENF	2.7	*S. frugiperda* Sf-9	Mutant R116A
TRMT10C-SDR5C1 complex	A/G_9	m^1A/G	cryo-EM	**8CBO**, 7ONU, 9EY0, 9EY1, 9EY2, 9GCH, 8CBK, 8CBL, 8CBM, 8RR3, 8RR4	3.2	*E. coli* BL21 (DE3) Rosetta/pRARE2/pRIL/ KRX strains	TRMT10C 40–403
ELP123 Elongator subcomplex	U_{34}	cm^5U	cryo-EM	**8PTX**, 8PTY, 8PTZ, 8PU0	2.9	*S. frugiperda* superSf9-3	Full-length
NSUN6	C_{72}	m^5C	X-ray	**5WWR**, 5WWS, 5WWT	3.1	*E. coli* Rosetta	Full-length
TRMT6/TRMT61A complex	A_{58}	m^1A	X-ray	**5CCB**, 5CCX, 5CD1	2.0	*E. coli* BL21 (DE3)	Full-length
METTL1-WDR4 complex	G_{46}	m^7G	cryo-EM	**8EG0**, 8D9K, 8D9L, 8CTH, 8CTI	3.5	*E. coli* Rosetta	Full-length
METTL6-SerRS complex	C_{32}	m^3C	cryo-EM	**8P7B**, 8P7C, 8P7D	2.4	*T. ni* Hi-5	Fusion construct

The PDB IDs of the depicted models are highlighted in bold, followed by PDB IDs of alternative structures. Abbreviations: X-ray crystallography (X-ray), Cryogenic electron microscopy (cryo-EM), *Escherichia coli* (*E. coli*), *Spodoptera frugiperda* (*S. frugiperda*), *Trichoplusia ni* (*T. ni*).

chromatography purification steps. The crystal structure of human PUS1 was determined at a resolution of 1.8 Å. PUS1 is a monomeric protein (~38 kDa) and exhibits a catalytic C-terminus and a central antiparallel β-sheet flanked by helices and loops (PDB ID 4IQM, Figure 1B).[43] Mitochondrial myopathy and sideroblastic anemia (MLASA) have been associated with human PUS1 dysfunction.[44,45]

RNA Pseudouridylate Synthase Domain-Containing 1 (RPUSD1)

Human RPUSD1 is a stand-alone enzyme that potentially modifies U_{20b}, U_{31}, U_{32}, e_{11-14}, U_{50} and U_{72} in tRNAs. The truncated construct of the human enzyme (residues 1–261) can be produced in *E. coli*. The obtained crystal structure at 1.9 Å resolution was determined by the Structural Genomics Consortium (SGC) showing a monomer (~30 kDa), with substantial similarity to the core region of other human PUS enzymes (PDB ID 5VBB, Figure 1C). It has been speculated that human RPUSD1 represents the homologue of yeast Pus6 or Pus9-like modification enzymes, but it has not been confirmed experimentally, yet.[46]

Pseudouridine Synthase 4 (PUS4)

Pseudouridine synthase 4 (TRUB1) modifies tRNA at position U_{55} alongside TRUB2 and PUS10 enzymes, resulting in the formation of Ψ_{55}.[47] The PUS4 crystallization construct (residues 58–318) was produced in frame with a 6xHis tag in the Rosetta (DE3) strain of *E. coli*. The monomeric human PUS4 protein (~29 kDa) was purified by IMAC and size exclusion chromatography and was shown to be active towards U_{54}/U_{55}-containing tRNAs. The crystal structure of PUS4 was determined at a resolution of 2.2 Å, showing the TruB domain, which contains an extended loop region with the stable KRKK motif utilized for RNA recognition (PDB ID 8JFX, Figure 1D).[48,49] Human PUS4 can suppress cellular proliferation rates by selective regulation of microRNA (miRNA) let-7 maturation. In detail, PUS4 was shown to bind the stem-loop structure of pri-miRNA (pri-let-7a1) independently of its enzymatic activity and thereby promote post-transcriptional gene silencing and suppress cell proliferation.[49]

Pseudouridine Synthase 7 (PUS7)

Human PUS7 is a TruD family member that can convert U_8, U_{13} and U_{35} of human tRNAs into Ψ. PUS7 is important for development and brain function,[50] but its overexpression can promote the development of colorectal cancer by stabilizing Sirtuin 1 (SIRT1) and activating the Wnt/β-catenin pathway.[51] The crystal structure of PUS7 has been solved at 2.3 Å resolution. The truncated expression construct (residues 99–661) has been cloned into the pET28-MHL vector and was expressed in the BL21 (DE3)-V3R-pRARE2 strain of *E. coli*. The protein was purified by IMAC, size exclusion chromatography and hydrophobic interaction chromatography. The structure of PUS7 shows a helix-turn-helix motif in the insertion C domain at its C-terminus, which likely contributes to tRNA binding, a catalytic aspartic acid residue (Asp294) and a so called R3H insertion (PDB ID 5KKP, Figure 1E).[50] The purified full length protein is monomeric with a molecular mass of ~65 kDa. N-terminal truncated PUS7 (Δ1–98) protein, missing the disordered N-terminus, binds tRNA and has similar pseudouridylation activity as the full length protein. Purified PUS7 modifies human $tRNA^{Ala}$ or a short 18-nucleotide fragment of $tRNA^{Gln}$ *in vitro,* while the PUS7 (Δ 1–98) D294A mutant has no catalytic activity. Moreover, the authors describe a model of PUS7 with the docked tRNA substrate.[50] Altered enzymatic activity of PUS7 and impaired pseudouridylation lead to plethora of neurodevelopmental disorders. Patients with a severe global developmental delay, epilepsy and progressive microcephaly have been linked to genomic variants of *PUS7* gene.[52,53]

Pseudouridine Synthase 10 (PUS10)

Human PUS10 catalyzes the formation of universally conserved Ψ_{54} and Ψ_{55} in tRNA.[54] Moreover, PUS10 has been shown to be important in TRAIL-induced apoptosis. The full length construct was expressed in the insect cells and purified by IMAC and size exclusion chromatography. Limited proteolysis of full length PUS10 with *Staphylococcus aureus* V8 protease resulted in the removal of a short loop region (i.e. residues 63 to 75), which enabled crystallization of PUS10 Δ63-75.[55] The crystal structure has been determined at a resolution of 2 Å. The structure of monomeric PUS10 (~61 kDa) shows a crescent-shaped molecule with two domains – the universally conserved catalytic PUS domain and a THUMP-containing domain, which is unique to the PUS10 family (PDB ID 2V9K, Figure 1F). The N-terminal RNA binding accessory domain (Met1–His285 Δ63-75) contains four conserved cysteine residues, which coordinate a zinc ion (Zn^{2+}). The active site resides in a deep pocket of a basic cleft, adjacent to a flexible thumb and forefinger loops of the C-terminal catalytic domain (Gly286–Asp528). PUS10 with its tRNA substrate has been modelled with the flipped out Ψ_{55} protruding into the active site of the enzyme, near the putative catalytic Asp344 residue.[55] PUS10 mutations are linked to

autoimmune diseases (celiac disease, ulcerative colitis) and intellectual disabilities in humans.[56–58]

Adenosine Deaminase Acting on tRNA 2 (ADAT2)

The adenosine-34-to-inosine deamination complex is formed by ADAT2 and ADAT3. It acts as a prerequisite for TRDMT1/DNMT2 recognition, which is linked to plethora of human cancers.[59] ADAT2 presents the ASL and complements the active site of ADAT3. The crystal structure of human tRNA-specific adenosine-34 deaminase subunit ADAT2 has been obtained at a resolution of 2.8 Å (PDB ID 3DH1, Figure 1G). The protein construct (residues 1–191) was expressed in bacteria, followed by IMAC, HRV-3C protease cleavage, ion exchange and size exclusion chromatography purification steps.[60] ADAT2 forms a homodimer with a mass of ~86 kDa and binds Zn^{2+} as a cofactor. The activity of the ADAT2 alone was not tested, but yeast and mouse ADAT complexes were shown to be active *in vitro*.[60] The ADAT2/ADAT3 complex is key for proper cortical development. Thus, any disturbances in its function cause neurodevelopmental disorders, including intellectual disability and microcephaly.[61,62]

AlkB Homolog 1 (ALKBH1)

ALKBH1 is an iron- (Fe^{2+}) and α-ketoglutarate-dependent dioxygenase. The human enzyme was reported to repair DNA by demethylating the N^6-methyladenine (m^6A) modification on DNA, but it is also involved in the biogenesis of 5-hydroxymethyl-2-O-methylcytidine (hm^5Cm) and 5-formyl-2-O-methylcytidine (f^5Cm) at position 34 in the anticodon of cytoplasmic and mitochondrial tRNAs.[63] A soluble construct (containing residues 1–389) can be expressed in the *E. coli* cells. The human ALKBH1 protein was purified by IMAC, followed by Tobacco Etch Virus (TEV) protease cleavage and size exclusion chromatography. The purified protein is a monomer of ~44 kDa and the crystal structure has been solved at 2 Å resolution (PDB ID 6IE3, Figure 1H). In comparison to other AlkB domain containing proteins, the structure of the Nucleotide Recognition Lid (NRL) of human ALKBH1 has several unique structural features, including a larger binding pocket over the central catalytic core that coordinates a manganese ion (Mn^{2+}) and an α-ketoglutarate (α-KG). Human ALKBH1 is active in demethylation assays *in vitro*.[64] ALKBH1 promotes tumorigenesis through depletion of DNA methylation levels in the genome and is a target for an anti-cancer drugs.[65,66]

AlkB Homolog 8 (ALKBH8)

Human ALKBH8 methylates 5-carboxymethyluridine (cm^5U) and 5-carboxylmethyl-2-thiouridine (cm^5s^2U) at the wobble position in the ASL of several tRNAs. Furthermore, it catalyzes the hydroxylation of the methylated 5-methoxycarbonylmethyluridine (mcm^5U_{34}) to form 5-methoxycarbonyl-1-hydroxymethyluridine ($mchm^5U_{34}$) in $tRNA^{Gly}_{UCC}$.[67] This final step in a rather complex tRNA modification cascade also requires the small accessory protein TRM112.[68] The crystal structure of the ALKBH8 RNA Recognition Motif (RRM) and AlkB domain was solved at a resolution of 3.2 Å. The crystallization construct (residues 25–354) with a 6xHis tag and TEV protease cleavage site was expressed in the B834 (DE3) strain of *E. coli* and purified by IMAC and size exclusion chromatography. The crystal structure of monomeric ALKBH8 (~40 kDa; PDB ID 3THP, Figure 1I) shows that both ALKBH8 domains are connected via a structured loop and that the AlkB domain coordinates Zn^{2+}, Mn^{2+} and α-KG.[69] In the presence of TRM112, ALKBH8 is active *in vitro* as shown by methyltransferase (MTase) activity assays.[68] The human ALKBH8 is linked to bladder cancer as it promotes cancer cell growth and progression.[70,71]

tRNA wybutosine-synthesizing protein 5 (TYW5)

TYW5, the tRNA yW-synthesizing enzyme 5, forms hydroxywybutosine (OHyW) on G_{37} by carbon hydroxylation, using $Fe(^{2+})$ ion and α-KG as cofactors. The homodimeric TYW5 (~156 kDa) was obtained after overexpression in the C41 (DE3) strain of *E. coli*. The recombinant protein was purified by IMAC, hydrophobic interaction and size exclusion chromatography steps. Expressing residues 1–311 of the human protein allowed crystallization and collection of diffraction data at 2.5 Å resolution, which revealed a novel JmjC (Jumonji C) domain fold (PDB ID 3AL5, Figure 1J).[72] The active site is positioned in the center of a β-jellyroll fold, a hallmark of the JmjC domains and other $Fe(^{2+})$/ α-KG-dependent oxygenases. TYW5 was crystallized with Mg^{2+} and α-KG or a nickel ion (Ni^{2+}) as cofactors. The homodimer is formed through a C-terminal helix bundle and possess hydroxylation activity *in vitro*.[72] JmjC proteins are implicated in breast cancer tumorigenesis, circadian rhythm regulation, embryological development and osteoclastogenesis.[73]

tRNA Aspartic Acid Methyltransferase 1 (TRDMT1)

TRDMT1 (or DNMT2) catalyzes the formation of 5-methylcytosine at position 38 (m^5C_{38}) in the anticodon loop of tRNAs – similarly to DNA cytosine-5-MTases.[59] The human glutathione-S-transferase (GST)-tagged protein lacking residues 191–237 (DNMT2Δ47) was expressed in the McrBC-deficient ER2488 strain of *E. coli* and

purified using a glutathione column, followed by thrombin cleavage and ion exchange chromatography (IEX) steps.[74] Purified DNMT2Δ47 elutes as a monomer with a mass of ~40 kDa that forms crystals in presence of S-Adenosyl-L-homocysteine (SAH) (PDB ID 1G55, Figure 1K), which diffracted to a resolution of 1.8 Å. The MTase activity was absent in the DNMT2Δ47 variant and very low for the purified full-length protein with DNA as a substrate.[74,75] However, TRDMT1 methylates the *C*5 atom of C_{38} in $tRNA^{Asp}_{GUC}$ and $tRNA^{Gly}_{GCC}$ using G_{34} as a discriminatory element. It further methylates $tRNA^{Val}_{AAC}$ and requires a priming A_{34}-to-I_{34} modification introduced by the ADAT2/ADAT3 complex.[59] The structure revealed sequence motifs that are conserved among m^5C MTases, including the consensus S-Adenosyl-L-methionine (SAM)-binding motif and a Pro-Cys dipeptide in the active site. DNMT2 has been reported to be related to human diseases, such as intellectual disability, gastric cancer, male infertility, and metabolic disorders.[59,76]

tRNA methyltransferase 2 homolog A (TRMT2A)

TRMT2A catalyzes the m^5U modification at position 54 and its depletion reduces translation fidelity.[77] The human enzyme was obtained by expressing the SUMO-tagged construct in the Rosetta strain of *E. coli*. The recombinant protein was purified by IMAC, HRV-3C protease cleavage and size exclusion chromatography purification steps.[77] The expressed RNA binding domain (RBD) of TRMT2A forms a homodimer (~10 kDa) without any bound cofactors (PDB ID 7NTO, Figure 1L). The crystal structure was determined at 1.2 Å resolution and revealed four anti-parallel β-strands and two α-helices that are packed against each other. The full-length protein, produced in insect cells, did not crystallized, but had MTase activity towards tRNA but not rRNA in luminescence-based MTase assays. Moreover, a TRMT2A–$tRNA^{Phe}$ AlphaFold model was experimentally validated by cross-linking mass spectrometry analyses, using full length TRMT2A and *in vitro* transcribed $tRNA^{Gln}$.[77] TRMT2A is associated with aggressive breast cancer with poor prognosis in patients with HER2 overexpression that are at an increased risk of tumor recurrence.[78]

TAR (HIV-1) RNA binding protein 1 (TARBP1)

Regulation of the HIV-1 (human immunodeficiency virus type-1) gene expression requires two regulatory elements: the *trans*-activator protein Tat and the transactivation-responsive region (TAR) downstream of the HIV-1 transcriptional initiation site.[79] TAR RNA forms a stable loop that binds RNA-binding proteins, like TARBP1, to regulate HIV replication. However, TARBP1 is also known to methylate the 2′-O-ribose moiety of G_{18} in some tRNAs. The expressed domain of human TARBP1 (residues 1438–1621) was cloned into the pET28a-LIC vector and expressed in the BL21 (DE3) Codon Plus RIL strain of *E. coli* strain.[80] The recombinant protein was purified via IMAC, followed by size exclusion chromatography, His-tag removal by thrombin cleavage and by IEX steps. The crystal structure of the MTase domain of human TARBP1 has been solved at a resolution of 1.6 Å (PDB ID 2HA8, Figure 1M). The MTase domain of TARBP1 forms a homodimer (~41 kDa) with two monomers in almost perpendicular arrangement. The catalytic core domain consists of six parallel β-strands packed between two layers of α-helices – forming a typical Rossmann fold with the C-terminus containing an unusual knot by threading the β6 strand through the β4– β5 loop. TARBP1 binds SAH in the pocket of two loops in the knotted region.[81] *In vitro* and *in vivo* Gm_{18} MTase activity has been experimentally confirmed for $tRNA^{Gln}_{UUG}$ and $tRNA^{Ser}_{UGA}$.[82] TARBP1 overexpression in NSCLC is associated with lung cancer, but it has also been linked to skin and liver cancer types and may be a prognostic marker.[82–84]

BCDIN3 domain containing RNA methyltransferase (BCDIN3D)

The bicoid interacting 3 domain containing RNA methyltransferase (BCDIN3D), is an evolutionarily conserved member of the Bin3 methyltransferase family. The human cytoplasmic $tRNA^{His}$-specific 5′-monomethylphosphate capping enzyme uses SAM as a methyl group donor.[85] A truncated construct (residue 14–284 with a loop deletion Δ92–99aa), was cloned into the pET-15b vector, expressed in the BL21 (DE3) strain of *E. coli* and purified by IMAC, heparin affinity and size exclusion chromatography steps (PDB ID 6L8U, Figure 1N).[86] The crystal structure of this BCDIN3D construct was solved at a resolution of 2.9 Å. The human BCDIN3D possess a classical Rossmann-fold, typical for MTases with the parallel β-sheet containing a topological switch in the center. The core of the structure is homologous to other human methyltransferases (MePCE, METTL16, NSUN6, TRMT61A and DNMT1).[86] It consists of seven β-strands (β1–β7) and six α-helices (α1–α6), and the β-strands form an extended β-sheet with the α-helices sandwiching both sides of the β-sheet (like MePCE, bound to SAH and RNAs). An *in vitro* methylation assay confirmed that the crystallized protein construct has 25% activity in comparison to the purified full-length/wild type BCDIN3D protein. The protein crystallized as a ~25 kDa monomer and a model with the docked tRNA has been calculated.[85] Of note, BCDIN3D overexpression is

associated with a tumorigenic phenotype and poor prognosis in breast cancer.[87,88]

Structures of human tRNA modifying enzymes in complex with tRNAs

In the second section, we would like to highlight those human tRNA modifying enzymes that have been structurally characterized in complex with substrate tRNAs (Figure 2, Figure 3 and Table 1). Not surprisingly single particle cryogenic electron microscopy (cryo-EM) is the dominating method of choice for the structure determination of these complex and highly dynamic assemblies.

tRNA guanine transglycosylase (TGT) complex

The human TGT complex is build up by two subunits, namely queuine tRNA-ribosyltransferase subunit 1 (QTRT1) and QTRT2. QTRT1 is the catalytically active subunit and it forms a heterodimer with QTRT2, which acts as an accessory subunit.[89–91] The QTRT1/QTRT2 complex is responsible for the incorporation of queuine into the wobble position 34 of four tRNAs, namely $tRNA^{Asn}_{GUU}$, $tRNA^{Asp}_{GUC}$, $tRNA^{His}_{GUG}$ and $tRNA^{Tyr}_{GUA}$, that contain a GUN anticodon (where N can be any nucleobase).[89,92] Queuosine (Q_{34}) modified $tRNA^{Asp}$ and $tRNA^{Tyr}$ can further be glycosylated by QTMAN, which adds mannose to Q_{34} in $tRNA^{Asp}$ and forms mannosyl-Q ($manQ_{34}$) and QTGAL which attaches galactose to Q_{34} in $tRNA^{Tyr}$ forming galactosyl-Q ($galQ_{34}$).[27] Eukaryotes cannot synthesize queuine *de novo* and rely on salvaging it from diet and/or the gut microbiome.[93] QTRT1/QTRT2 binds queuine and its target tRNA, followed by excising G_{34} and the formation of a covalent intermediate between the catalytic aspartate in QTRT1 and the abasic ribose. This intermediate is resolved through the formation of an N-glycosidic bond between queuine and the ribose 34 generating queuosine.[94] The structure of the human QTRT1/QTRT2 complex bound to Zn^{2+}, *in vitro*-transcribed $tRNA^{Asp}$ and 9–deazaguanine, an inhibitory analog of guanine, which stabilizes the intermediate state, was solved at an overall resolution of 2.9 Å using cryo-EM (PDB ID 8OMR; Figure 2A).[95] Human QTRT1, with an N-terminal 6xHis tag and HRV–3C protease cleavage site, and QTRT2 were cloned into a bacterial pCDF Duet1 co-expression vector and transformed into the *E. coli* BL21 (DE3) strain. The expressed proteins were subjected to IMAC purification, tag removal by protease cleavage and size exclusion chromatography.[95] The QTRT1/QTRT2 complex was reconstituted with *in vitro*-transcribed $tRNA^{Asp}$ and an excess of 9-deazaguanine. After an incubation of 20 h on ice, the reconstituted complex was subjected to an additional size exclusion chromatography step before preparation of cryo-EM grids.[95] The overall structure of the QTRT1/QTRT2 complex resembles a previously determined crystal structure of the complex bound to an anticodon stem loop hairpin.[89] QTRT1 and QTRT2 both harbor a central $(\beta/\alpha)_8$ barrel with insertions and a zinc binding domain, which are characteristic for the TGT protein family.[89,95] Both proteins dimerize mainly through their zinc binding domains.[89] The tRNA lies on top of the complex, with the elbow region pointing away from it. QTRT2 binds the tRNA core via three binding motifs, an β3βE turn together with the N-terminal half of α4 helix bind to the 3′ strand of the acceptor stem and an βEβF sheet interacts with the base of the D-arm.[95] The anticodon stem loop is distorted and bound in the active site of QTRT1 in a similar manner to the crystal structure.[89,95] The abasic ribose 34 is in proximity of the catalytic aspartate and 9-deazaguanine.[95] It was shown that patients with ovarian and lung cancer had reduced Q_{34}-modification levels and a poor survival prognosis.[93] Other studies observed that higher expression of QTRT1 is favorable prognostic marker for cervical cancer, but an unfavorable one for renal cancer. Loss of or hypomodification of Q_{34} have been also linked to reduced mRNA translation in mitochondria during oxidative stress and dysregulation of aerobic respiration, which can promote cancer proliferation.[96,97]

Pseudouridine Synthase 3 (PUS3)

In humans, the pseudouridylation of tRNA at positions 38 and 39 is facilitated by the pseudouridine synthase 3 (PUS3).[98,99] The structures of mutant PUS3 variants in the apo (PDB ID 9F9Q) and tRNA-bound states (PDB ID 8OKD, 9ENC and 9ENB with $tRNA^{Gln}$; PDB ID 9ENE with $tRNA^{Arg}$; PDB ID 9ENF with pre-$tRNA^{Arg}$) were solved by cryo–EM. PUS3 R116A bound to two $tRNA^{Gln}$ molecules was solved at an overall resolution of 2.7 Å (PDB ID 9ENB, Figure 2B). For the expression of full-length PUS3 (∼55 kDa) in Sf9 insect cells, a pFastBac backbone was used, which included an additional GST-tag at the N-terminus. Purification was performed using affinity chromatography with a glutathione column, followed by a final size exclusion chromatography polishing step. The analytical gel filtration profiles for both the wild type and catalytic mutants, namely R116A and D118A, showed the formation of stable homodimers. PUS3 contains a conserved PUS domain, which is flanked by eukaryotic-specific extensions at the N- and C-terminus. Moreover, the solved structure revealed a distinct interface for the PUS3 homodimer, exhibiting an antiparallel coiled coil interaction to stabilize the PUS3 monomers via conserved residues at the C-terminus (338–369) in both, apo and tRNA bound structures. The tRNA bound models revealed that both of the bound tRNAs contact each of the PUS3 monomer – one contact is made at the elbow region (D- and T-

arm) and one at the ASL regions, which positioned the modified U_{38}/U_{39} in close proximity of the PUS3 active site.[100] The modification plays a significant role in tRNA stability and function. Mutations associated with PUS3 have been extensively studied and are implicated in the neurodevelopmental disorders, like intellectual disability.[101,102,38,99]

Mitochondrial TRMT10C/SDR5C1 complex

The human m^1R_9 (R = purine) tRNA methyltransferase 10 (TRMT10) family consists of 3 members, namely TRMT10A, TRMT10B and TRMT10C.[103] All three enzymes are part of the SPOUT MTase superfamily and utilize SAM as a methyl-group donor.[104] TRMT10A specifically methylates *N*1 of G_9 in a subset of nucleo-cytoplasmatic tRNAs,[105,106] whereas TRMT10B selectively methylates *N*1 of A_9 of nuclear encoded $tRNA^{Asp}_{GUC}$.[105,106] It is currently not known whether TRMT10A or TRMT10B act as a standalone MTase or require a partner protein for their target specificity *in vivo*.[105] Mitochondrial TRMT10C in complex with four short-chain dehydrogenase/reductase 5C1 (SDR5C1) subunits serves as a tRNA-binding

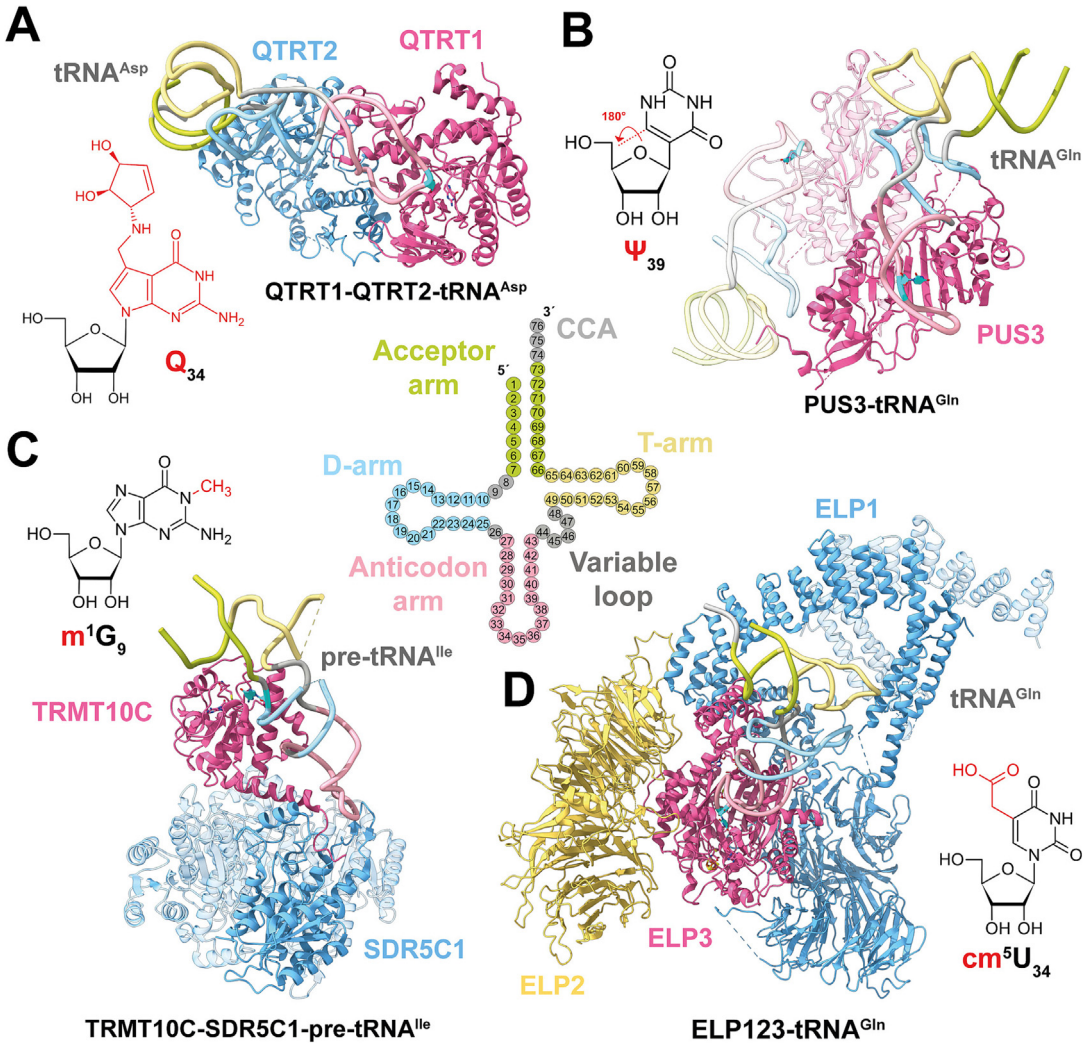

Figure 2. Structures of human tRNA modifying protein complexes. Representative structures of human tRNA modifiers in complex with their target tRNAs, solved by cryo-EM are shown. A clover leaf representation of the tRNA is shown in the center, specific regions are colored as follows: acceptor arm (light green), D-arm (light blue), anticodon arm (light pink), variable arm (grey), T-arm (yellow) and 3′CCA tail (light grey). The catalytic subunits are colored in soft pink and the accessory subunits are colored in sky blue and yellow. All bound tRNAs are colored according to the clover leaf model and modification sites are highlighted in cyan. Chemical structures of modified nucleosides are displayed next to the complex and the modification is highlighted in red. (A) QTRT1-QTRT2-$tRNA^{Asp}$ (PDB ID 8OMR), (B) $PUS3_{R116A}$-$tRNA^{Gln}$ (PDB ID 9ENB), (C) $TRMT10_{40-403}$-SDR5C1-pre-$tRNA^{Ile}$ (PDB ID 8CBO), (D) ELP123-$tRNA^{Gln}$ (PDB ID 8PTX).

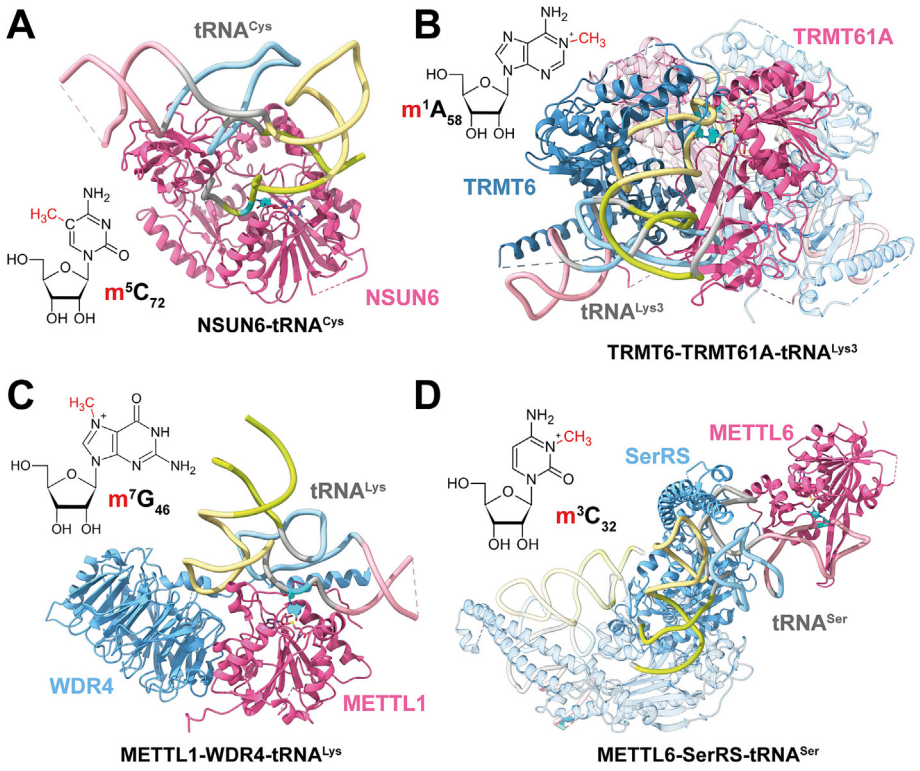

Figure 3. Models of cytosolic human tRNA methyltransferase complexes. Representative structural models of tRNA bound methyltransferases solved by cryo-EM or crystallography are displayed. Bound tRNAs and modified bases are colored as described in Figure 2. The color scheme for the protein complexes is soft pink for catalytic subunits and sky blue for the partner subunit. In case of TRMT6-TMT61A and METTL6-SerRS one dimer is colored as described previously and the second dimer is colored in a darker shade, to visualize the tRNA binding mode of the hetero tetrameric protein complexes (see text). The chemical structure of the modified nucleoside and the position are shown next to the model, the added methyl-moiety is highlighted in red. (A) NSUN6-tRNA^{Cys} (PDB ID 5WWR), (B) TRMT6-TRMT61A-tRNA^{Lys3} (PDB ID 5CCB), (C) METTL1-WDR4-tRNA^{Lys} (PDB ID 8EG0), (D) METLL6-SerRS-tRNA^{Ser} (PDB ID 8P7B).

platform for the sequential mitochondrial tRNA (mt-tRNA) maturation process, by 5′- and 3′-processing of pre-tRNA by RNase P (PRORP) and RNase Z (ELAC2) as well as the subsequent 3′-CCA addition by TRNT1.[107–110] Of note, the crystal structure of bacterially expressed TRNT1 by itself was determined at 1.9 Å resolution. The structure reveals a four-domain architecture (head, neck, body, tail) with a cluster of conserved residues forming a positively charged cleft between the first two domains.[111] Studies have demonstrated that unlike the highly specific TRMT10A and TRMT10B enzymes, TRMT10C shows dual specificity and methylates *N*1 of position 9 in 19 out of 22 mt-tRNAs.[103,105] Methylation of this position in tRNA blocks a potential Watson-Crick pairing and prevents a misfolding of tRNA, as shown for mt-tRNA^{Lys}, where the unmodified tRNA forms an alternative, non-functional extended stem-loop structure.[112,113] Of note, TRMT10C requires the presence of the partner protein SDRC51C for efficient tRNA methylation activity.[103] Recently, several groups have determined structures of the human mt-tRNA maturation machinery using single particle cryo-EM (PDB IDs 7ONU, 9EY0, 9GCH, 8CBK, 8CBL, 8CBM, 8RR3).[108–110,114] In the appreciation of other review articles, we focus here only on the MTase subcomplex consisting of only TRMT10C and SDRC51C (PDB ID 8CBO). All groups have followed a similar expression and purification approach. TRMT10C lacking the first 40 amino acids (containing the mitochondrial targeting sequence) was cloned in-frame after a 6xHis tag and TEV protease cleavage site in a bacterial expression vector. To co-express the subcomplex, full length SDRC51C was cloned after TRMT10C and spaced with a ribosome-binding site to create a polycistronic translation cassette.[103,108,110,115] The subcomplex was expressed in *E. coli* BL21 (DE3) derived strains (e.g. Rosetta) or carrying a plasmid with rare tRNAs (e.g. pRARE2, pRIL) or in the *E. coli* KRX strain.[108–110] Proteins were purified by IMAC, IEX, heparin chromatography, removal of the tag by TEV cleavage and size exclusion chromatography. Cryo-EM sample preparation for the pre-tRNA bound TRMT10C-SDRC51C complex, was achieved by reconstitution of the co-purified subcomplex with

in vitro transcribed pre-tRNA and the cofactors SAH and nicotinamide adenine dinucleotide (NADH), before vitrification.[108] The group solved the structure of the pre-tRNA bound complex at an overall resolution of 3.2 Å (PDB ID 8CBO, Figure 2C).[108] Four SDRC51C subunits form a flat symmetric tetramer that serves as a platform for up to two TRMT10C copies. Both TRMT10C molecules are bound to pre-tRNA and are located on opposing sides of the tetramer, forming a hexameric protein complex of ~195 kDa.[115] TRMT10C is comprised of an N-terminal domain (NTD), an adaptor region and a MTase domain. Whereas SDR5C1 consists only of a dehydrogenase domain. TRMT10C binds at the top of the SDR51C tetramer via its adaptor region and the C-terminal part of its MTase domain.[108–110] tRNA binding by the subcomplex is achieved mainly through TRMT10C and both domains are involved. TRMT10C forms an extensive interaction with the tRNA, the NTD binds to the tRNA on the opposite side of the MTase domain and interacts with the variable loop and the D- and T-arm. The adapter region loops around the ASL and stabilizes it together with SDR5C1. The MTase domain of TRMT10C forms interactions with the D- and the anticodon-arms. The acceptor stem of the pre-tRNA lies on top of the MTase domain and is accessible to the tRNA maturation machinery.[108–110] The SAM or SAH bound active site of TRMT10C points towards the substrate base, which is flipped in and the *N*1-R_9 position is in proximity of the bound cofactor.[108–110] Defects in the mitochondrial MTase subcomplex can lead to several mitochondrial dysfunctions, as it can affect the mt-tRNA maturation machinery. Mutations in TRMT10C and SDR5C1 are associated among others with cardiomyopathy, intellectual disabilities, neurodegeneration, microcephaly and lactic acidosis.[37] We recommend an excellent review that summarizes the recent progress in understanding the structure and function of the complex.[116]

ELP123 subcomplex of Elongator

Elongator is a highly conserved dodecameric complex, consisting of two copies of each of the six Elongator proteins (ELP1-ELP6) that form two discrete subcomplexes, termed ELP123 and ELP456, respectively.[117,118] The ELP123 subcomplex is catalytic active and the hexameric ring-shaped ELP456 subcomplex appears to fulfill only a regulatory function.[119,120] Elongator introduces a priming 5-carboxymethyl (cm^5) group at wobble uridines (U_{34}) in the anticodon of 13 different cytoplasmatic tRNAs in humans.[117,121] The ELP3 subunit catalyzes this reaction in a SAM and acetyl coenzyme A (acetyl-CoA) dependent manner.[122] This pivotal cm^5U_{34} modification, serves as a starting point for other enzymes that further modify the cm^5U to mcm^5U, $mchm^5U$, 5-methoxycarbonylmethyl-2-thiouridine (mcm^5s^2U), 5-methoxycarbonylmethyl-2′-O-methyluridine (mcm^5Um), 5-carbamoylmethyluridine (ncm^5U) or carbamoylmethyl-2′-O-methyluridine (ncm^5-Um).[117,121] Our group recently solved the cryo-EM structure of the human ELP123 subcomplex bound to *in vitro*-transcribed $tRNA^{Gln}$, acetyl-CoA and the SAM cleavage products 5-deoxyadenosyl (5′-dA) and methionine at an overall resolution of 2.9 Å (PDB ID 8PTX; Figure 2D).[117] The codon optimized open reading frames of ELP1, ELP2 and ELP3 (tagged with a C-terminal Twin-Strep sequence) were clone into a pBIG1a vector using Gibson assembly. The proteins were expressed in superSf9-3 insect cells, purified via a streptavidin-based column, followed by heparin chromatography and size exclusion chromatography steps. The ELP123 complex was incubated with *in vitro* transcribed $tRNA^{Gln}$, in presence of acetyl-CoA and SAM, and vitrified.[117] The human ELP123 subcomplex of ~610 kDa resembles the 2-lobed structure of previously solved eukaryotic Elp123 complexes, from yeast and mouse.[117,120] Each lobe consists of one ELP1, ELP2 and ELP3 subunit bound to one tRNA. ELP1 serves as a scaffold for the other subunits, it dimerizes at its C-terminus and forms an arch-like structure. The two N-terminal WD40 domains of ELP1 and both WD40 domains of ELP2 clamp the ELP3 subunit between each other.[117] ELP3 possesses two functional domains, an N-terminal radical SAM (rSAM) with an iron-sulfur cluster and a C-terminal lysine acetyltransferase (KAT) domain.[117] tRNA binding by the ELP123 subcomplex is achieved through ELP1 and ELP3. ELP3 binds and distorts the ASL in its central catalytic cleft, where U_{33} and U_{34} are flipped out of the anticodon loop. U_{33} is pointing towards the bound acetyl-CoA in the KAT domain and U_{34} is in proximity of the iron-sulfur cluster of the rSAM domain. The non-conserved N-terminal extension of ELP3, consisting of three helix bundle, contacts the tRNA anticodon arm with the first two helices and the third helix stabilizes the deformed anticodon loop. ELP1 contacts the tRNA elbow region via a stretch of basic residues in the C-terminal tetratricopeptide domain.[117] It was shown that ELP3′s acetyl-CoA hydrolysis activity is only triggered in presence of its target tRNAs, but not by previously suspected histone peptides. Furthermore, U_{33} is not only positioned in the center of ELP3, but it is also essential for acetyl-CoA hydrolysis *in vitro* and *in vivo*. However, the cm^5U_{34} modification could not be reconstituted *in vitro*, yet.[117,120] Several human diseases are linked to mutations in the Elongator complex, including neurodegenerative disorders and different forms of cancer.[123]

Nucleolar S-phase Ubiquitin-like 6 (NSUN6)

The human MTase NSUN6 catalyzes the m^5C modification in tRNAs at position 72 (C_{72}), which is located at the 3′ end of the tRNA acceptor

stem. NSUN6 facilitates the modification of specific *iso*-acceptors, namely $tRNA^{Cys}$ and $tRNA^{Thr}$.[124] The crystal structure of apo (PDB ID 5WWQ) and $tRNA^{Cys}$ bound (PDB ID 5WWT) were solved at 2.8 Å and 3.2 Å respectively. In addition, two more $tRNA^{Cys}$ bound structures were solved in the presence of the methyl group donor SAM (PDB ID 5WWS) and its inhibiting analog, sinefungin (SFG; PDB ID 5WWR; Figure 3A) at 3.3 Å and 3.1 Å respectively.[125] A pET22b vector backbone containing a 6xHis tag at the C-terminus was utilized for the expression of NSUN6 (~52 kDa) in the Rosetta strain of *E. coli* cells. Purification of the expressed protein was achieved through IMAC, followed by a final polishing step using size exclusion chromatography.[126] Structurally, NSUN6 encompasses a non-conserved N-terminal extension comprising three alpha-helices and a ~60-residue RRM. Its catalytic core features a canonical MTase domain that is homologous to other members of the RNA:m^5C MTase family. The family shares a Rossmann fold, spanning approximately 250 residues, along with a ~90-residue pseudouridine synthase and archaeosine transglycosylase (PUA) domain insertion connected by two linkers. The binding of tRNA to NSUN6 does not alter the arrangement of the MTase and PUA domains, while engaging tRNA primarily through its acceptor- and D-arms. However, the acceptor arm of tRNA undergoes significant conformational changes upon binding. The bases from U_{71}-U_{76} form a U-turn to expose the base of C_{72} for its modification while simultaneously engaging with the diverse domains of the NSUN6 protein. Interestingly, the structural integrity remains largely unaffected by the presence of additional ligands, such as SAM and SFG in the presence of tRNA.[125] NSUN6 has been reported to methylate Hippo/MST1 while activating YAP1 in the downstream pathway, which constitutes a major regulator for bone metastasis, making it as an excellent therapeutic target against aggressive tumors.[125,127]

TRMT6/TRMT61A complex

The cytosolic m^1A_{58} methyltransferase complex consists of the smaller catalytic subunit TRMT61A and the larger RNA-binding module TRMT6. Both subunits form a heterodimer which assemble further into a hetero-tetramer.[128] TRMT6 and TRMT61A share a similar structure with an N-terminal β-sheet domain, which is connected via a flexible linker region to a C-terminal domain with a typical Rossmann-fold.[128] The complex needs to recognize multiple substrates as it is responsible for catalyzing the m^1A_{58} modification in nearly all human tRNAs, using SAM as a methyl donor.[33,129] The crystal structure of TRMT6-TRMT61A in complex with *in vitro* transcribed $tRNA^{Lys3}$ and SAH was obtained at a 2.0 Å resolution (PDB ID 5CCB; Figure 3B).[128] TRMT6 with a C-terminal HRV-3C protease cleavage site and a 6xHis tag was co-overexpressed with TRMT61A in bacteria. Subsequently, the complex was purified via IMAC, followed by tag cleavage with HRV-3C protease and size exclusion chromatography.[128] Each heterodimer, in the tetrameric complex, forms a L-shaped positively charged surface that accommodates one tRNA molecule. tRNA binding is achieved by TRMT61A from the first heterodimer and TRMT6 from the second heterodimer and *vice versa*.[128] The complex deforms the elbow region of the tRNA, by opening the base pairing between G_{18} and G_{19} in the D-loop and U_{55} and C_{56} in the T-loop, to expose A_{58}.[128] This distortions position A_{58} in proximity of the SAH-bound active site of TRMT61A. The anticodon arm is stabilized by loop regions in the CTD of TRMT6 and the acceptor stem is bound by the NTD of TRMT61A.[128] In humans, higher expression levels of TRMT6 and TRMT61A and elevated m^1A_{58} methylation activity are linked to urothelial carcinoma of the bladder and hepatocellular carcinomas.[130,131]

Methyltransferase-like protein 1/WDR4 complex

The Methyltransferase-like protein 1 (METTL1) – WD Repeat Domain 4 (WDR4) complex methylates the *N7* position of G_{46} in the variable loop of various human tRNAs.[5,132] METTL1 is the catalytical subunit and consists of an N-terminal tail, followed by the catalytic core domain with a Rossmann-like fold, typical for class I MTases.[133,134] WDR4 is the accessory subunit that serves as a scaffold for tRNA and METTL1 and consists of seven WD40 repeats that adopt a 7-bladed β-propeller structure with a C-terminal helix.[133,134] m^7G_{46} introduces a positive charge in the variable loop that facilitates the triple base pairing with C_{13} and G_{22} in the D-loop, which increases the stability of the tertiary tRNA structure.[34] Two groups have independently solved the tRNA-bound structure of the METTL1-WDR4 complex in presence and absence of a cofactor SAM or SAH by single particle cryo-EM.[133,134] Both groups obtained a higher resolved structure when they incubated the protein complex with tRNA and SAH. Ruiz-Arroyo *et al.* solved the METTL1-WDR4 complex with *in vitro*-transcribed $tRNA^{Lys}$ at an overall resolution of 3.5 Å (PDB ID 8EG0; Figure 3C) and Li *et al.* used fully modified $tRNA^{Phe}$ to solve the structure at 3.3 Å resolution (PDB ID 8CTH).[133,134] Both groups followed a similar cloning, expression and purification strategy. They cloned both human genes into the bacterial co-overexpression pETDuet vector and after expression, purified the protein complex by IMAC, followed by IEX and size exclusion chromatography – of note, one group performed an additional heparin chromatography step before size exclusion chromatography step.[133,134] Complex reconstitution was achieved by incubation of the purified

METTL1-WDR4 with tRNA and SAH. Subsequently, the ternary complex was applied directly on grids, or it was re-purified by size exclusion chromatography before vitrification.[133,134] WDR4 faces METTL1 with its WD40 domains 2 to 5, which are highly conserved in eukaryotes.[133,134] Both complexes interact with the tRNA, WDR4 contacts the T-arm of the tRNA with WD40 domains 3 and 4 and its C-terminal helix interact with the D-arm. METTL1 recognizes the variable loop and binds also with the elbow region.[133,134] By comparing the structure of METTL1-WDR4-tRNA^{Lys} to the SAH-bound structure, the authors observed that G_{46} flips out of the variable loop, which is promoted by the N-terminal tail and is positioned closer into the active site of METTL1 in proximity of SAH.[133] Furthermore, both groups noticed that the unstructured N-terminal tail becomes ordered in presence of the cofactor and tRNA. The N-terminus becomes sandwiched between the catalytic loop of METTL1 and C-terminal helix of WDR4, it stabilizes the catalytic loop, contacts the tRNA and coordinates the C-terminal helix of WDR4, which strengthens tRNA binding by both proteins.[133,134] In addition, both groups proposed a model for the previously described regulation of METTL1 through phosphorylation of serine 27 (Ser27). Phosphorylation of Ser27 inactivates the methylation activity and both groups suggest, that the negatively charged phosphate group would create a steric clash and charge repulsion in the catalytic center.[133–135] Mutations or dysregulation of METTL1 and WDR4 have been associated with cancer, developmental defects, neurological and metabolic disorders in humans.[38,33]

Methyltransferase-like protein 6/seryl-tRNA synthase complex

Human METTL6 belongs to the METTL family and is responsible for the m^{3}C$_{32}$ methylation of tRNA^{Ser} in the cytosol, together with the seryl-tRNA synthase (SerRS).[136,137] It was demonstrated that METTL6 on its own can selectively methylate *in vitro* transcribed tRNA$^{Ser}_{UGA}$ in a SAM-dependent manner, but not tRNA$^{Thr}_{CGU}$ which is targeted by METTL2A/B.[136–139] The methylation activity of METTL6 increase by ~1000-fold upon addition of SerRS.[138] Throll *et al.* have recently solved the structure of a SerRS-METTL6 fusion construct bound to tRNA^{Ser} at an overall resolution of 2.4 Å using single particle cryo-EM (PDB ID 8P7B; Figure 3D).[138] The group initially attempted to reconstitute the complex from individual components but failed to obtain a complex that remained stably associated during grid preparation.[138] Hence, they cloned the coding sequence of METTL6, including an N-terminal linker, between SerRS and the C-terminal HRV-3C protease cleavage site and EGFP tag. Subsequently, they expressed the fusion construct in *Trichoplusia ni* Hi-5 insect cells and purified it using an EGFP nanobody resin. They eluted the protein by HRV-3C protease cleavage, subjected it to size exclusion chromatography and collected complex containing fractions that co-purified with tRNA^{Ser} from the expression host. The complex was diluted into a buffer containing the MTase inhibitor sinefungin and applied on grids.[138] Structural analyses show that two SerRS copies dimerize via their aminoacylation domain (AD) and are bound with up to two tRNA molecules. SerRS of one subunit recognizes the target tRNA via the NTD stalk that binds in the cleft between T-arm and the unique long variable loop of tRNA^{Ser}. The 3′end of the tRNA acceptor stem points towards SerRS AD of the second subunit, but is not fully bound in the active site.[138] Although METTL6 was fused to the C-terminus of SerRS, not all classes of SerRS showed a density for METTL6, suggesting that the chosen linker in principle allows for the dissociation of METTL6.[138] METTL6 forms a canonical Rossmann-fold and consists of the catalytic MTase core domain and m^{3}C methyltransferase-specific RNA-binding domain (m^{3}C-RBD).[138,140] The tripartite m^{3}C-RBD is spread around the core domain and is formed by the N-terminal region, internal insertion and a hairpin β-extensions, consisting of an antiparallel β6–β7 sheet.[138,140] Only two loops from SerRS NTD form an interaction with two helices in the N-terminal region of METTL6.[138] METTL6 binds tRNA^{Ser} through the positively charged m^{3}C-RBD. This leads to a structural rearrangement and causes a rigidification of the disordered m^{3}C-RDB region.[138] The anticodon arm of tRNA^{Ser} is bend towards METTL6 upon binding. C_{32} is flipped out from the anticodon loop and is stabilized by m^{3}C-RBD and methyltransferase core domain and the modified *N*3-C_{32} atom is in close distance to the sulfur atom of SAH.[138] Furthermore, the authors observed that the co-purified tRNA^{Ser}, carried an *N*6-isopentenyl modification at position A_{37} (i^{6}A$_{37}$), which was coordinated by residues in the insertion and β-extensions region of the m^{3}C-RBD.[138] It was shown that disturbances in METTL6 expression level affect translation, cell homeostasis, tumorigenesis and development.[141,142]

Structurally still uncharacterized human tRNA modification enzymes

In summary, research groups have so far experimentally determined structures of 22 different human tRNA modification enzymes, including several clinically highly relevant proteins. Despite the recent progress in the field, we are still lacking experimental structures for the majority of human tRNA modifying enzymes. Since the advent of high confidence structural modeling,[143] determining structures of single proteins (or at least protein domains), appears to become an expensive academic exercise. It is not surprising that AlphFold3[144] is able to provide high-confidence models for the core regions in most of the missing

human tRNA enzymes. In particular, enzymes that belong to protein families where the structure of another member or a closely related eukaryotic/-mammalian homologue is available. For this reason, the missing structures of human dihydrouridine synthases (DUS1, DUS3, DUS4L)[145] PUS7L[146] the tRNA-specific adenosine deaminases (ADAT1, ADAT3), the isopentenyltransferase TRIT1,[147] the acetyltransferase NAT10,[148] the aminocarboxypropyltransferases (DTWD1/ DTWD2)[149] and several MTases and MTase-adaptor complexes (TRMT1L, TRMT5, TRMT10B, TRMT13, THUMPD3/TRMT112, TRM11/TRMT112, METTL2A/DALRD3, METTL2B/DALRD3, FTSJ1/THADA, FTSJ1/WDR6, TRMT44, TRMO, NSUN2) can be predicted with high confidence. In addition, the pathway components that lead to the synthesis of wybutosine have been characterized in archaea.[150] Even if little is known about CDKAL and the most recently identified RNA glycosylases,[27] the three-dimensional structures can be predicted. However, the identity of the human enzymes that are responsible for the following modifications m^1A_{14}, m^3C_{20}, $\Psi m/Gm_{39}$, $m^1\Psi_{39}$, m^5C_{40}, $\Psi_{e11\text{-}14}$, $Um_{e11\text{-}14}$ and m^5Um_{54} remain unknown[38,151] and therefore not even the best prediction algorithm will be able to provide detailed structural insights. Furthermore, we are still missing the enzymes that are responsible for generating the ncm^5U_{34} downstream of Elongator[152] and the enzyme that converts wybutosine into peroxywybutosine ($o2yW_{37}$). Of note, it is not clear if these modification reactions are catalysed by yet unknown enzymes or whether known enzymes are repurposed. Finally, we are lacking information for the two larger modification complexes in humans, namely the CTU1/CTU2 thiotransferase complex and the KEOPS complex.

CTU1/CTU2 complex

The URM1/MOCS3 pathway is responsible for catalyzing s^2-thiouridine formation on U_{34} in four human tRNAs.[153] In detail, $tRNA^{Lys}_{UUU}$, $tRNA^{Glu}_{UUC}$, $tRNA^{Gln}_{UUG}$ and $tRNA^{Arg}_{UCU}$ that have undergone a preceding modification on the *C*5 position by the Elongator complex,[152] receive a sulfur (thiol) on their *C*2 position, resulting in a $mcm^5s^2U_{34}$ modified wobble base. Six proteins responsible for 2-thiouridine formation in eukaryotes have been identified by different groups.[153–155] In detail, the L-cysteine desulferase and sulfur donor NFS1[156] initially activates and supplies sulfur atoms to the cascade. The sulfur (persulfide) is then transferred either directly, or via MPST to the rhodanese-like domain of MOCS3. Subsequently, MOCS3 activates URM1 and transfers the persulfide group to the C-terminus of URM1. During the final step of the cascade, sulfur is passed onto the wobble base uridine via the tRNA binding CTU1/CTU2 thioltransferase complex.[157] The primary sequences of CTU1/CTU2 are evolutionary highly conserved. Both subunits share a common fold, which is highly similar to TtuA, which is responsible for the ATP-dependent 2-thiolation of U_{54} in some archaeal tRNAs.[158] The atomic structure of the TtuA homodimers has recently been studied intensively.[159–163] Considering the stark differences between TtuA and CTU1/CTU2, the current knowledge about thiolation in humans (and other eukaryotes) remains rather speculative. The malfunction of the human tRNA thiolation pathway is associated with DREAM-PL syndrome[164–166] and specific pathogenic *CTU2* variants are causally linked to the development of the disease.

KEOPS complex

The cytoplasmatic human KEOPS complex (Kinase, Endopeptidase and Other Proteins of Small size) consists of five subunits, namely OSGEP (Kae1), TP53RK (Bud32), TPRKB (Cgi121), LAGE3 (Pcc1) and GON7.[167–169] The KEOPS complex is responsible for installing a threonylcarbamoyl moiety at the *N*6 position of A_{37} (t^6A_{37}) in ANN decoding tRNAs (where N can be any nucleobase).[170] t^6A_{37} is an essential and universally conserved tRNA modification.[171] It prevents a Watson-Crick pairing between U_{33} and A_{37}, thereby stabilizing the seven nucleotide anticodon loop formation and is required for translational fidelity and reading frame maintenance.[172,173] The catalytic subunit OSGEP uses the precursor threonylcarbamoyl adenylate (TC-AMP), which is synthesized by the similarly conserved protein YRDC (Sua5), and transfers the TC-group onto adenosine. However, in the cytosol this reaction apparently also requires the fully assembled KEOPS complex.[171] Based on composite models using the crystal structures of human OSGEP-LAGE3-Gon7 (PDB ID 6GWJ) and TP53RK-TPRKB (PDB ID 6WQX) it was proposed that the complex has a linear overall organization.[168,169] OSGEP resides between LAGE3 and the atypical kinase TP53RK, TPRKB interacts with TP53RK and GON7 is bound to LAGE3 on the opposite of OSGEP.[167,169] It was further demonstrated that the KEOPS complex can form dimers via a homodimerization interface in a LAGE3 (in absence of GON7) and that this dimerization results in a 2:2:2:2 stoichiometry of the complex.[167] Recently, two groups could determine the cryo-EM structures of the KEOPS complexes from archaea and *Arabidopsis thaliana* (*A. thaliana*).[174,175] For archaeal KEOPS in its apo and tRNA bound state, Chuquimarca *et al.* used a Pcc1 mutant that cannot dimerize the KEOPS complex but retains tRNA t^6A modification activity and omitted Gon7 in the reconstitution reaction.[174] Zheng *et al.* reconstituted *A. thaliana* Kae1, Pcc1, Bud32 and Cgi121 and solved the structure of the dimeric KEOPS complex.[175] Mutations in the KEOPS complex are linked to neurological disor-

ders like microcephaly and Galloway-Mowat syndrome, nephrotic defects and cancer.[38,176]

Future Perspectives

Macromolecular crystallography has dominated the field and delivered the vast majority of structural information for human tRNA modifying enzymes, namely for 16 out of 22 human enzymes. For instance, all presented individual structures of apo proteins have been determined by crystallography, but only two of the tRNA-bound structures (i.e. NSUN6 and TRM6/TRM61A complex) were resolved by crystallography. Most structures of human multi-subunit complexes and tRNA-bound enzymes have been obtained by single particle cryo-EM. This is caused by several technical reasons. (i) Highly dynamic assemblies are less likely to form crystal lattices. (ii) It is more feasible to obtain smaller quantities of highly pure samples for cryo-EM than large sample quantities required for macromolecular crystallography or nuclear magnetic resonance spectroscopy (NMR). (iii) The chances of obtaining well-diffracting crystals for a biological macromolecule is increased by focusing on defined structural domains and truncating flexible regions and loops, which could be involved in tRNA binding and subunit interactions. (iv) The increasing availability of high-end cryogenic electron microscopes around the world has facilitated the access and collection of large high-quality datasets. (v) Improvements in data analyses tools for cryo-EM and the access to high performance computational clusters has enabled a larger community to determine high resolution cryo-EM structures on a regular basis.

The method required strongly reduced quantities of high quality tRNA preparations and also offers the opportunity to isolate human enzymes (and complexes) from native source (e.g. human cell lines). In agreement, the samples for the most recent cryo-EM structures have been mainly produced by co-expression in insect cells using sophisticated co-expression systems (e.g. biGBac).[177] Of note, the subsequent purification protocols are still similar, but to avoid dissociation of the subunits or the bound tRNA molecules, harsh buffer conditions and high salt concentrations are mostly avoided. Finally, the use of mild cross-linking reagents (often used to stabilize multi-subunit protein complexes during vitrification) could have detrimental consequences for tRNA binding and are mostly avoided. Once the sample is purified, cryo-EM allows to use similar sample preparation conditions for similar samples, which facilitates structure determination of the same human enzyme with different tRNAs and with different ligands (e.g. SAM, SAH). Hence, it becomes easier to solve a cascade of structures of different reaction intermediates without the laborious (and mostly unsuccessful), resource demanding search for crystallization conditions for each slightly altered sample of interest.

Despite the improvement in predicting proteins, protein complexes and protein-DNA complexes,[143,144] predicting the fold of RNA molecules and the assembly of protein-(t)RNA complexes still remains extremely challenging.[178] In our own experience, the predicted position of the tRNA molecules in the tRNA-bound complexes is often modeled with low confidence and the obtained models often orientate the modified nucleotide outside of the anticipated active site of the enzyme. Furthermore, the list of the top-ranked models of tRNA-bound complexes often contains models with tRNA molecules bound in different locations or different orientations (confusing acceptor stem and anticodon stem and loop), respectively. Hence, single particle cryo-EM not only offers an excellent opportunity to study highly dynamic tRNA modifying enzymes and complexes, but it is still required to obtain experimental structural information to infer molecular details about those complexes.

We are excited about the new opportunities that structural predictions and single particle cryo-EM offer to the field of tRNA biology and we are curious to see the next fascinating structures awaiting to be released.

CRediT authorship contribution statement

Alexander Hammermeister: Writing – original draft, Visualization, Supervision, Investigation, Data curation, Conceptualization. **Monika Gaik:** Writing – original draft, Visualization, Investigation, Data curation, Conceptualization. **Priyanka Dahate:** Writing – original draft, Visualization, Investigation, Data curation, Conceptualization. **Sebastian Glatt:** Writing – original draft, Supervision, Investigation, Funding acquisition, Data curation, Conceptualization.

DATA AVAILABILITY

No data was used for the research described in the article.

DECLARATION OF COMPETING INTEREST

The authors declare that they have no known competing financial interests or personal relationships that could have appeared to influence the work reported in this paper.

Acknowledgement

We thank the members of the Glatt lab for vivid discussion and suggestions. This project has

received funding from the European Research Council (ERC) under the European Union's Horizon 2020 research and innovation programme (grant agreement No. 101001394).

Received 14 January 2025;
Accepted 22 March 2025;
Available online 10 April 2025

Keywords:
tRNA modifications;
modifying enzymes;
cryo-EM;
protein complexes;
tRNA

† These authors contributed equally.

References

1. Lane, B.G., (2014). Historical perspectives on RNA nucleoside modifications. *In: Modification and editing of RNA*. https://doi.org/10.1128/9781555818296.ch1.
2. McCown, P.J., Ruszkowska, A., Kunkler, C.N., Breger, K., Hulewicz, J.P., Wang, M.C., Springer, N.A., Brown, J.A., (2020). Naturally occurring modified ribonucleosides. *Wiley Interdiscip. Rev. RNA* **11**, e1595.
3. Jackman, J.E., Alfonzo, J.D., (2013). Transfer RNA modifications: nature's combinatorial chemistry playground. *Wiley Interdiscip. Rev. RNA* **4**, 35–48. https://doi.org/10.1002/wrna.1144.
4. Motorin, Y., Helm, M., (2010). tRNA stabilization by modified nucleotides. *Biochemistry* **49**, 4934–4944. https://doi.org/10.1021/bi100408z.
5. Cappannini, A., Ray, A., Purta, E., Mukherjee, S., Boccaletto, P., Moafinejad, S.N., Lechner, A., Barchet, C., Klaholz, B.P., Stefaniak, F., Bujnicki, J.M., (2024). MODOMICS: a database of RNA modifications and related information. 2023 update. *Nucleic Acids Res.* **52**, D239–D244. https://doi.org/10.1093/nar/gkad1083.
6. Dunin-Horkawicz, S., Czerwoniec, A., Gajda, M.J., Feder, M., Grosjean, H., Bujnicki, J.M., (2006). MODOMICS: a database of RNA modification pathways. *Nucleic Acids Res.* **34**, D145–D149. https://doi.org/10.1093/nar/gkj084.
7. Phizicky, E.M., Hopper, A.K., (2010). tRNA biology charges to the front. *Genes Dev.* **24**, 1832–1860. https://doi.org/10.1101/gad.1956510.
8. Crick, F.H., (1958). On protein synthesis. *Symp. Soc. Exp. Biol.* **12**, 138–163.
9. Holley, R.W., Apgar, J., Everett, G.A., Madison, J.T., Marquisee, M., Merrill, S.H., Penswick, J.R., Zamir, A., (1965). Structure of a ribonucleic acid. *Science (1979)* **147**, 1462–1465. https://doi.org/10.1126/science:147.3664.1462.
10. Chan, P.P., Lowe, T.M., (2016). GtRNAdb 2.0: an expanded database of transfer RNA genes identified in complete and draft genomes. *Nucleic Acids Res.* **44**, D184–D189. https://doi.org/10.1093/nar/gkv1309.
11. Giegé, R., Jühling, F., Pütz, J., Stadler, P., Sauter, C., Florentz, C., (2012). Structure of transfer RNAs: similarity and variability. *Wiley Interdiscip. Rev. RNA* **3**, 37–61. https://doi.org/10.1002/wrna.103.
12. Krutyhołowa, R., Zakrzewski, K., Glatt, S., (2019). Charging the code — tRNA modification complexes. *Curr. Opin. Struct. Biol.* **55**, 138–146. https://doi.org/10.1016/j.sbi.2019.03.014.
13. Behrens, A., Rodschinka, G., Nedialkova, D.D., (2021). High-resolution quantitative profiling of tRNA abundance and modification status in eukaryotes by mim-tRNAseq. *Mol. Cell* **81**, 1802–1815.e7. https://doi.org/10.1016/j.molcel.2021.01.028.
14. Kellner, S., Neumann, J., Rosenkranz, D., Lebedeva, S., Ketting, R.F., Zischler, H., Schneider, D., Helm, M., (2014). Profiling of RNA modifications by multiplexed stable isotope labelling. *Chem. Commun. (Camb.)* **50**, 3516–3518. https://doi.org/10.1039/c3cc49114e.
15. Begik, O., Lucas, M.C., Pryszcz, L.P., Ramirez, J.M., Medina, R., Milenkovic, I., Cruciani, S., Liu, H., Vieira, H. G.S., Sas-Chen, A., Mattick, J.S., Schwartz, S., Novoa, E. M., (2021). Quantitative profiling of pseudouridylation dynamics in native RNAs with nanopore sequencing. *Nature Biotechnol.* **39**, 1278–1291. https://doi.org/10.1038/s41587-021-00915-6.
16. Helm, M., Motorin, Y., (2017). Detecting RNA modifications in the epitranscriptome: predict and validate. *Nature Rev. Genet.* **18**, 275–291. https://doi.org/10.1038/nrg.2016.169.
17. Motorin, Y., Helm, M., (2024). General principles and limitations for detection of RNA modifications by sequencing. *Acc. Chem. Res.* **57**, 275–288. https://doi.org/10.1021/acs.accounts.3c00529.
18. Kristen, M., Lander, M., Kilz, L.-M., Gleue, L., Jörg, M., Bregeon, D., Hamdane, D., Marchand, V., Motorin, Y., Friedland, K., Helm, M., (2024). DORQ-seq: high-throughput quantification of femtomol tRNA pools by combination of cDNA hybridization and Deep sequencing. *Nucleic Acids Res.* **52**, e89.
19. Schultz, S.K.L., Kothe, U., (2020). tRNA elbow modifications affect the tRNA pseudouridine synthase TruB and the methyltransferase TrmA. *RNA* **26**, 1131–1142. https://doi.org/10.1261/RNA.075473.120.
20. Lorenz, C., Lünse, C.E., Mörl, M., (2017). tRNA modifications: impact on structure and thermal adaptation. *Biomolecules* **7** https://doi.org/10.3390/biom7020035.
21. Barraud, P., Gato, A., Heiss, M., Catala, M., Kellner, S., Tisné, C., (2019). Time-resolved NMR monitoring of tRNA maturation. *Nature Commun.* **10**, 3373. https://doi.org/10.1038/s41467-019-11356-w.
22. Rozov, A., Demeshkina, N., Khusainov, I., Westhof, E., Yusupov, M., Yusupova, G., (2016). Novel base-pairing interactions at the tRNA wobble position crucial for accurate reading of the genetic code. *Nature Commun.* **7**, 10457. https://doi.org/10.1038/ncomms10457.
23. Ranjan, N., Rodnina, M.V., (2016). tRNA wobble modifications and protein homeostasis. *Translation (Austin)* **4**, e1143076. https://doi.org/10.1080/21690731.2016.1143076.
24. Rodnina, M.V., Fischer, N., Maracci, C., Stark, H., (2017). Ribosome dynamics during decoding. *Philos. Trans. R. Soc. Lond. B Biol. Sci.* **372** https://doi.org/10.1098/rstb.2016.0182.
25. Rezgui, V.A., Tyagi, K., Ranjan, N., Konevega, A.L., Mittelstaet, J., Rodnina, M.V., Peter, M., Pedrioli, P.G., (2013). tRNA tKUUU, tQUUG, and tEUUC wobble position modifications fine-tune protein translation by

promoting ribosome A-site binding. *PNAS* **110**, 12289–12294. https://doi.org/10.1073/pnas.1300781110.
26. Vendeix, F.A.P., Dziergowska, A., Gustilo, E.M., Graham, W.D., Sproat, B., Malkiewicz, A., Agris, P.F., (2008). Anticodon domain modifications contribute order to tRNA for ribosome-mediated codon binding. *Biochemistry* **47**, 6117–6129. https://doi.org/10.1021/bi702356j.
27. Zhao, X., Ma, D., Ishiguro, K., Saito, H., Akichika, S., Matsuzawa, I., Mito, M., Irie, T., Ishibashi, K., Wakabayashi, K., Sakaguchi, Y., Yokoyama, T., Mishima, Y., Shirouzu, M., Iwasaki, S., Suzuki, T., Suzuki, T., (2023). Glycosylated queuosines in tRNAs optimize translational rate and post-embryonic growth. *Cell* **186**, 5517–5535.e24. https://doi.org/10.1016/j.cell.2023.10.026.
28. Ranjan, N., Rodnina, M.V., (2017). Thio-modification of tRNA at the wobble position as regulator of the kinetics of decoding and translocation on the ribosome. *J. Am. Chem. Soc.* **139**, 5857–5864. https://doi.org/10.1021/jacs.7b00727.
29. Rodnina, M.V., (2016). The ribosome in action: tuning of translational efficiency and protein folding. *Protein Sci.* **25**, 1390–1406. https://doi.org/10.1002/pro.2950.
30. Nedialkova, D.D., Leidel, S.A., (2015). Optimization of codon translation rates via tRNA modifications maintains proteome integrity. *Cell* **161**, 1606–1618. https://doi.org/10.1016/j.cell.2015.05.022.
31. Agris, P.F., Narendran, A., Sarachan, K., Vare, V.Y.P., Eruysal, E., (2017). The importance of being modified: the role of RNA modifications in translational fidelity. *Enzymes (Essen)* **41**, 1–50. https://doi.org/10.1016/bs.enz.2017.03.005.
32. Novoa, E.M., Pavon-Eternod, M., Pan, T., Ribas de Pouplana, L., (2012). A role for tRNA modifications in genome structure and codon usage. *Cell* **149**, 202–213. https://doi.org/10.1016/j.cell.2012.01.050.
33. de Crécy-Lagard, V., Boccaletto, P., Mangleburg, C.G., Sharma, P., Lowe, T.M., Leidel, S.A., Bujnicki, J.M., (2019). Matching tRNA modifications in humans to their known and predicted enzymes. *Nucleic Acids Res.* **47**, 2143–2159. https://doi.org/10.1093/nar/gkz011.
34. Biela, A., Hammermeister, A., Kaczmarczyk, I., Walczak, M., Koziej, L., Lin, T.-Y., Glatt, S., (2023). The diverse structural modes of tRNA binding and recognition. *J. Biol. Chem.* **299**, 104966. https://doi.org/10.1016/j.jbc.2023.104966.
35. Lai, L.B., Lai, S.M., Szymanski, E.S., Kapur, M., Choi, E. K., Al-Hashimi, H.M., Ackerman, S.L., Gopalan, V., (2022). Structural basis for impaired 50 processing of a mutant tRNA associated with defects in neuronal homeostasis. *PNAS* **119**, e2119529119. https://doi.org/10.1073/pnas.2119529119.
36. Delaunay, S., Helm, M., Frye, M., (2024). RNA modifications in physiology and disease: towards clinical applications. *Nature Rev. Genet.* **25**, 104–122. https://doi.org/10.1038/s41576-023-00645-2.
37. Orellana, E.A., Siegal, E., Gregory, R.I., (2022). tRNA dysregulation and disease. *Nature Rev. Genet.* **23**, 651–664. https://doi.org/10.1038/s41576-022-00501-9.
38. Suzuki, T., (2021). The expanding world of tRNA modifications and their disease relevance. *Nature Rev. Mol. Cell Biol.* **22**, 375–392. https://doi.org/10.1038/s41580-021-00342-0.
39. Whelan, F., Jenkins, H.T., Griffiths, S.C., Byrne, R.T., Dodson, E.J., Antson, A.A., (2015). From bacterial to human dihydrouridine synthase: automated structure determination. *Acta Crystallogr. D Biol. Crystallogr.* **71**, 1564–1571. https://doi.org/10.1107/S1399004715009220.
40. Bou-Nader, C., Pecqueur, L., Bregeon, D., Kamah, A., Guérineau, V., Golinelli-Pimpaneau, B., Guimarães, B.G., Fontecave, M., Hamdane, D., (2015). An extended dsRBD is required for post-transcriptional modification in human tRNAs. *Nucleic Acids Res.* **43**, 9446–9456. https://doi.org/10.1093/nar/gkv989.
41. Byrne, R.T., Jenkins, H.T., Peters, D.T., Whelan, F., Stowell, J., Aziz, N., Kasatsky, P., Rodnina, M.V., Koonin, E.V., Konevega, A.L., Antson, A.A., (2015). Major reorientation of tRNA substrates defines specificity of dihydrouridine synthases. *PNAS* **112**, 6033–6037. https://doi.org/10.1073/pnas.1500161112.
42. Kato, T., Daigo, Y., Hayama, S., Ishikawa, N., Yamabuki, T., Ito, T., Miyamoto, M., Kondo, S., Nakamura, Y., (2005). A novel human tRNA-dihydrouridine synthase involved in pulmonary carcinogenesis. *Cancer Res.* **65**, 5638–5646. https://doi.org/10.1158/0008-5472.CAN-05-0600.
43. Czudnochowski, N., Wang, A.L., Finer-Moore, J., Stroud, R.M., (2013). In human pseudouridine synthase 1 (hPus1), a C-terminal helical insert blocks tRNA from binding in the same orientation as in the Pus1 bacterial homologue TruA, consistent with their different target selectivities. *J. Mol. Biol.* **425**, 3875–3887. https://doi.org/10.1016/j.jmb.2013.05.014.
44. Bykhovskaya, Y., Casas, K., Mengesha, E., Inbal, A., Fischel-Ghodsian, N., (2004). Missense mutation in pseudouridine synthase 1 (PUS1) causes mitochondrial myopathy and sideroblastic anemia (MLASA). *Am. J. Hum. Genet.* **74**, 1303–1308. https://doi.org/10.1086/421530.
45. Patton, J.R., Bykhovskaya, Y., Mengesha, E., Bertolotto, C., Fischel-Ghodsian, N., (2005). Mitochondrial myopathy and sideroblastic anemia (MLASA): missense mutation in the pseudouridine synthase 1 (PUS1) gene is associated with the loss of tRNA pseudouridylation. *J. Biol. Chem.* **280**, 19823–19828. https://doi.org/10.1074/jbc.M500216200.
46. Behm-Ansmant, I., Grosjean, H., Massenet, S., Motorin, Y., Branlant, C., (2004). Pseudouridylation at position 32 of mitochondrial and cytoplasmic tRNAs requires two distinct enzymes in *Saccharomyces cerevisiae*. *J. Biol. Chem.* **279**, 52998–53006. https://doi.org/10.1074/jbc.M409581200.
47. Mukhopadhyay, S., Deogharia, M., Gupta, R., (2021). Mammalian nuclear TRUB1, mitochondrial TRUB2, and cytoplasmic PUS10 produce conserved pseudouridine 55 in different sets of tRNA. *RNA* **27**, 66–79. https://doi.org/10.1261/rna.076810.120.
48. Xuan, Y., Wang, L., Zhang, L., Lv, M., Li, F., Gong, Q., (2024). Structural basis of pri-let-7 recognition by human pseudouridine synthase TruB1. *Biochem. Biophys. Res. Commun.* **721**, 150122. https://doi.org/10.1016/j.bbrc.2024.150122.
49. Kurimoto, R., Chiba, T., Ito, Y., Matsushima, T., Yano, Y., Miyata, K., Yashiro, Y., Suzuki, T., Tomita, K., Asahara, H., (2020). The tRNA pseudouridine synthase TruB1 regulates the maturation of let-7 miRNA. *EMBO J.* **39**, 1–19. https://doi.org/10.15252/embj.2020104708.

50. Guegueniat, J., Halabelian, L., Zeng, H., Dong, A., Li, Y., Wu, H., Arrowsmith, C.H., Kothe, U., (2021). The human pseudouridine synthase PUS7 recognizes RNA with an extended multi-domain binding surface. *Nucleic Acids Res.* **49**, 11810–11822. https://doi.org/10.1093/nar/gkab934.
51. Zhang, Q., Fei, S., Zhao, Y., Liu, S., Wu, X., Lu, L., Chen, W., (2023). PUS7 promotes the proliferation of colorectal cancer cells by directly stabilizing SIRT1 to activate the Wnt/β-catenin pathway. *Mol. Carcinog.* **62**, 160–173. https://doi.org/10.1002/mc.23473.
52. Shaheen, R., Tasak, M., Maddirevula, S., Abdel-Salam, G.M.H., Sayed, I.S.M., Alazami, A.M., Al-Sheddi, T., Alobeid, E., Phizicky, E.M., Alkuraya, F.S., (2019). PUS7 mutations impair pseudouridylation in humans and cause intellectual disability and microcephaly. *Hum. Genet.* **138**, 231–239. https://doi.org/10.1007/s00439-019-01980-3.
53. Han, S.T., Kim, A.C., Garcia, K., Schimmenti, L.A., Macnamara, E., Network, U.D., Gahl, W.A., Malicdan, M.C., Tifft, C.J., (2022). PUS7 deficiency in human patients causes profound neurodevelopmental phenotype by dysregulating protein translation. *Mol. Genet. Metab.* **135**, 221–229. https://doi.org/10.1016/j.ymgme.2022.01.103.
54. Deogharia, M., Mukhopadhyay, S., Joardar, A., Gupta, R., (2019). The human ortholog of archaeal Pus10 produces pseudouridine 54 in select tRNAs where its recognition sequence contains a modified residue. *RNA* **25**, 336–351. https://doi.org/10.1261/rna.068114.118.
55. McCleverty, C.J., Hornsby, M., Spraggon, G., Kreusch, A., (2007). Crystal structure of human Pus10, a novel pseudouridine synthase. *J. Mol. Biol.* **373**, 1243–1254. https://doi.org/10.1016/j.jmb.2007.08.053.
56. Festen, E.A.M., Goyette, P., Green, T., Boucher, G., Beauchamp, C., Trynka, G., Dubois, P.C., Lagacé, C., Stokkers, P.C.F., Hommes, D.W., Barisani, D., Palmieri, O., Annese, V., van Heel, D.A., Weersma, R.K., Daly, M. J., Wijmenga, C., Rioux, J.D., (2011). A meta-analysis of genome-wide association scans identifies IL18RAP, PTPN2, TAGAP, and PUS10 as shared risk loci for crohn's disease and celiac disease. *PLoS Genet.* **7**, 3–8. https://doi.org/10.1371/journal.pgen.1001283.
57. Medrano, L.M., Pascual, V., Bodas, A., López-Palacios, N., Salazar, I., Espino-Paisán, L., González-Pérez, B., Urcelay, E., Mendoza, J.L., Núñez, C., (2019). Expression patterns common and unique to ulcerative colitis and celiac disease. *Ann. Hum. Genet.* **83**, 86–94. https://doi.org/10.1111/ahg.12293.
58. Chen, C.P., Chern, S.R., Wu, P.S., Chen, S.W., Lai, S.T., Chuang, T.Y., Chen, W.L., Yang, C.W., Wang, W., (2018). Prenatal diagnosis of a 3.2-Mb 2p16.1-p15 duplication associated with familial intellectual disability. *Taiwan. J. Obstet. Gynecol.* **57**, 578–582. https://doi.org/10.1016/j.tjog.2018.06.018.
59. Huang, Z.X., Li, J., Xiong, Q.P., Li, H., Wang, E.D., Liu, R. J., (2021). Position 34 of tRNA is a discriminative element for m5C38 modification by human DNMT2. *Nucleic Acids Res.* **49**, 13045–13061. https://doi.org/10.1093/nar/gkab1148.
60. Ramos-Morales, E., Bayam, E., Del-Pozo-Rodríguez, J., Salinas-Giegé, T., Marek, M., Tilly, P., Wolff, P., Troesch, E., Ennifar, E., Drouard, L., Godin, J.D., Romier, C., (2021). The structure of the mouse ADAT2/ADAT3 complex reveals the molecular basis for mammalian tRNA wobble adenosine-to-inosine deamination. *Nucleic Acids Res.* **49**, 6529–6548. https://doi.org/10.1093/nar/gkab436.
61. Alazami, A.M., Hijazi, H., Al-Dosari, M.S., Shaheen, R., Hashem, A., Aldahmesh, M.A., Mohamed, J.Y., Kentab, A., Salih, M.A., Awaji, A., Masoodi, T.A., Alkuraya, F.S., (2013). Mutation in ADAT3, encoding adenosine deaminase acting on transfer RNA, causes intellectual disability and strabismus. *J. Med. Genet.* **50**, 425–430. https://doi.org/10.1136/jmedgenet-2012-101378.
62. Del-Pozo-Rodriguez, J., Tilly, P., Lecat, R., Vaca, H.R., Mosser, L., Brivio, E., Balla, T., Gomes, M.V., Ramos-Morales, E., Schwaller, N., Salinas-Giegé, T., VanNoy, G., England, E.M., Lovgren, A.K., O'Leary, M., Chopra, M., Ojeda, N.M., Toosi, M.B., Eslahi, A., Alerasool, M., Mojarrad, M., Pais, L.S., Yeh, R.C., Gable, D.L., Hashem, M.O., Abdulwahab, F., Alzaidan, H., Aldhalaan, H., Tous, E., Alsagheir, A., Alowain, M., Tamim, A., Alfayez, K., Alhashem, A., Alnuzha, A., Kamel, M., Al-Awam, B.S., Elnaggar, W., Almenabawy, N., O'Donnell-Luria, A., Neil, J.E., Gleeson, J.G., Walsh, C.A., Alkuraya, F.S., AlAbdi, L., Elkhateeb, N., Selim, L., Srivastava, S., Nedialkova, D. D., Drouard, L., Romier, C., Bayam, E., Godin, J.D., (2024). Neurodevelopmental disorders associated variants in ADAT3 disrupt the activity of the ADAT2/ADAT3 tRNA deaminase complex and impair neuronal migration. *MedRxiv*. https://doi.org/10.1101/2024.03.01.24303485.
63. Kawarada, L., Suzuki, T., Ohira, T., Hirata, S., Miyauchi, K., Suzuki, T., (2017). ALKBH1 is an RNA dioxygenase responsible for cytoplasmic and mitochondrial tRNA modifications. *Nucleic Acids Res.* **45**, 7401–7415. https://doi.org/10.1093/nar/gkx354.
64. Tian, L.F., Liu, Y.P., Chen, L., Tang, Q., Wu, W., Sun, W., Chen, Z., Yan, X.X., (2020). Structural basis of nucleic acid recognition and 6mA demethylation by human ALKBH1. *Cell Res.* **30**, 272–275. https://doi.org/10.1038/s41422-019-0233-9.
65. Le Xiao, C., Zhu, S., He, M., Chen, D., Zhang, Q., Chen, Y., Yu, G., Liu, J., Xie, S.Q., Luo, F., Liang, Z., Wang, D. P., Bo, X.C., Gu, X.F., Wang, K., Yan, G.R., (2018). N6-methyladenine DNA modification in the human genome. *Mol. Cell* **71**, 306–318.e7. https://doi.org/10.1016/j.molcel.2018.06.015.
66. Xie, Q., Wu, T.P., Gimple, R.C., Li, Z., Prager, B.C., Wu, Q., Yu, Y., Wang, P., Wang, Y., Gorkin, D.U., Zhang, C., Dowiak, A.V., Lin, K., Zeng, C., Sui, Y., Kim, L.J.Y., Miller, T.E., Jiang, L., Lee-Poturalski, C., Huang, Z., Fang, X., Zhai, K., Mack, S.C., Sander, M., Bao, S., Kerstetter-Fogle, A.E., Sloan, A.E., Xiao, A.Z., Rich, J.N., (2018). N6-methyladenine DNA modification in glioblastoma. *Cell* **175**, 1228–1243.e20. https://doi.org/10.1016/j.cell.2018.10.006.
67. Fu, Y., Dai, Q., Zhang, W., Ren, J., Pan, T., He, C., (2010). The AlkB domain of mammalian ABH8 catalyzes hydroxylation of 5-methoxycarbonylmethyluridine at the wobble position of tRNA. *Angew. Chem. Int. Ed. Engl.* **49**, 8885–8888. https://doi.org/10.1002/anie.201001242.
68. Songe-Møller, L., van den Born, E., Leihne, V., Vågbø, C. B., Kristoffersen, T., Krokan, H.E., Kirpekar, F., Falnes, P.Ø., Klungland, A., (2010). Mammalian ALKBH8 possesses tRNA methyltransferase activity required for the biogenesis of multiple wobble uridine modifications

implicated in translational decoding. *Mol. Cell Biol.* **30**, 1814–1827. https://doi.org/10.1128/mcb.01602-09.
69. Pastore, C., Topalidou, I., Forouhar, F., Yan, A.C., Levy, M., Hunt, J.F., (2012). Crystal structure and RNA binding properties of the RNA recognition motif (RRM) and AlkB domains in human AlkB homolog 8 (ABH8), an enzyme catalyzing tRNA hypermodification. *J. Biol. Chem.* **287**, 2130–2143. https://doi.org/10.1074/jbc.M111.286187.
70. Shimada, K., Nakamura, M., Anai, S., De Velasco, M., Tanaka, M., Tsujikawa, K., Ouji, Y., Konishi, N., (2009). A novel human AlkB homologue, ALKBH8, contributes to human bladder cancer progression. *Cancer Res.* **69**, 3157–3164. https://doi.org/10.1158/0008-5472.CAN-08-3530.
71. Ohshio, I., Kawakami, R., Tsukada, Y., Nakajima, K., Kitae, K., Shimanoe, T., Saigo, Y., Hase, H., Ueda, Y., Jingushi, K., Tsujikawa, K., (2016). ALKBH8 promotes bladder cancer growth and progression through regulating the expression of survivin. *Biochem. Biophys. Res. Commun.* **477**, 413–418. https://doi.org/10.1016/j.bbrc.2016.06.084.
72. Kato, M., Araiso, Y., Noma, A., Nagao, A., Suzuki, T., Ishitani, R., Nureki, O., (2011). Crystal structure of a novel JmjC-domain-containing protein, TYW5, involved in tRNA modification. *Nucleic Acids Res.* **39**, 1576–1585. https://doi.org/10.1093/nar/gkq919.
73. Del Rizzo, P.A., Krishnan, S., Trievel, R.C., (2012). Crystal structure and functional analysis of JMJD5 indicate an alternate specificity and function. *Mol. Cell Biol.* **32**, 4044–4052. https://doi.org/10.1128/mcb.00513-12.
74. Dong, A., Yoder, J.A., Zhang, X., Zhou, L., Bestor, T.H., Cheng, X., (2001). Structure of human DNMT2, an enigmatic DNA methyltransferase homolog that displays denaturant-resistant binding to DNA. *Nucleic Acids Res.* **29**, 439–448. https://doi.org/10.1093/nar/29.2.439.
75. Hermann, A., Schmitt, S., Jeltsch, A., (2003). The human Dnmt2 has residual DNA-(cytosine-C5) methyltransferase activity. *J. Biol. Chem.* **278**, 31717–31721. https://doi.org/10.1074/jbc.M305448200.
76. Yang, X.X., He, X.Q., Li, F.X., Wu, Y.S., Gao, Y., Li, M., (2012). Risk-association of DNA methyltransferases polymorphisms with gastric cancer in the Southern Chinese population. *Int. J. Mol. Sci.* **13**, 8364–8378. https://doi.org/10.3390/ijms13078364.
77. Witzenberger, M., Burczyk, S., Settele, D., Mayer, W., Welp, L.M., Heiss, M., Wagner, M., Monecke, T., Janowski, R., Carell, T., Urlaub, H., Hauck, S.M., Voigt, A., Niessing, D., (2023). Human TRMT2A methylates tRNA and contributes to translation fidelity. *Nucleic Acids Res.* **51**, 8691–8710. https://doi.org/10.1093/nar/gkad565.
78. Hicks, D.G., Janarthanan, B.R., Vardarajan, R., Kulkarni, S.A., Khoury, T., Dim, D., Budd, G.T., Yoder, B.J., Tubbs, R., Schreeder, M.T., Estopinal, N.C., Beck, R.A., Wang, Y., Ring, B.Z., Seitz, R.S., Ross, D.T., (2010). The expression of TRMT2A, a novel cell cycle regulated protein, identifies a subset of breast cancer patients with HER2 over-expression that are at an increased risk of recurrence. *BMC Cancer* **10** https://doi.org/10.1186/1471-2407-10-108.
79. Weeks, K.M., Ampe, C., Schultz, S.C., Steitz, T.A., Crothers, D.M., (1990). Fragments of the HIV-1 Tat protein specifically bind TAR RNA. *Science* **249**, 1281–1285. https://doi.org/10.1126/science:2205002.
80. Wu, H., Min, J., Zeng, H., Plotnikov, A.N., (2008). Crystal structure of the methyltransferase domain of human TARBP1. *Proteins: Struct. Funct. Genet.* **72**, 519–525. https://doi.org/10.1002/prot.22065.
81. Wu, H., Min, J., Zeng, H., Plotnikov, A.N., (2008). Crystal structure of the methyltransferase domain of human TARBP1. *Proteins* **72**, 519–525. https://doi.org/10.1002/prot.22065.
82. Shi, X., Zhang, Y., Wang, Y., Wang, J., Gao, Y., Wang, R., Wang, L., Xiong, M., Cao, Y., Ou, N., Liu, Q., Ma, H., Cai, J., Chen, H., (2024). The tRNA Gm18 methyltransferase TARBP1 promotes hepatocellular carcinoma progression via metabolic reprogramming of glutamine. *Cell Death Differ.* **31**, 1219–1234. https://doi.org/10.1038/s41418-024-01323-4.
83. Sand, M., Skrygan, M., Georgas, D., Arenz, C., Gambichler, T., Sand, D., Altmeyer, P., Bechara, F.G., (2012). Expression levels of the microRNA maturing microprocessor complex component DGCR8 and the RNA-induced silencing complex (RISC) components argonaute-1, argonaute-2, PACT, TARBP1, and TARBP2 in epithelial skin cancer. *Mol. Carcinog.* **51**, 916–922. https://doi.org/10.1002/mc.20861.
84. Ye, J., Wang, J., Zhang, N., Liu, Y., Tan, L., Xu, L., (2018). Expression of tarbp1 protein in human non-small-cell lung cancer and its prognostic significance. *Oncol. Lett.* **15**, 7182–7190. https://doi.org/10.3892/ol.2018.8202.
85. Martinez, A., Yamashita, S., Nagaike, T., Sakaguchi, Y., Suzuki, T., Tomita, K., (2017). Human BCDIN3D monomethylates cytoplasmic histidine transfer RNA. *Nucleic Acids Res.* **45**, 5423–5436. https://doi.org/10.1093/nar/gkx051.
86. Liu, Y., Martinez, A., Yamashita, S., Tomita, K., (2020). Crystal structure of human cytoplasmic tRNAHis-specific 5-monomethylphosphate capping enzyme. *Nucleic Acids Res.* **48**, 1572–1582. https://doi.org/10.1093/NAR/GKZ1216.
87. Yao, L., Chi, Y., Hu, X., Li, S., Qiao, F., Wu, J., Shao, Z. M., (2016). Elevated expression of RNA methyltransferase BCDIN3D predicts poor prognosis in breast cancer. *Oncotarget* **7**, 53895–53902. https://doi.org/10.18632/oncotarget.9656.
88. Liu, R., Wang, X., Chen, G.Y., Dalerba, P., Gurney, A., Hoey, T., Sherlock, G., Lewicki, J., Shedden, K., Clarke, M.F., (2007). The prognostic role of a gene signature from tumorigenic breast-cancer cells. *N. Engl. J. Med.* **356**, 217–226. https://doi.org/10.1056/NEJMoa063994.
89. Sievers, K., Welp, L., Urlaub, H., Ficner, R., (2021). Structural and functional insights into human tRNA guanine transgylcosylase. *RNA Biol.* **18**, 382–396. https://doi.org/10.1080/15476286.2021.1950980.
90. Behrens, C., Biela, I., Petiot-Bécard, S., Botzanowski, T., Cianférani, S., Sager, C.P., Klebe, G., Heine, A., Reuter, K., (2018). Homodimer architecture of QTRT2, the noncatalytic subunit of the eukaryotic tRNA-guanine transglycosylase. *Biochemistry* **57**, 3953–3965. https://doi.org/10.1021/ACS.BIOCHEM.8B00294.
91. Chen, Y.C., Kelly, V.P., Stachura, S.V., Garcia, G.A., (2010). Characterization of the human tRNA-guanine transglycosylase: confirmation of the heterodimeric

subunit structure. *RNA* **16**, 958–968. https://doi.org/10.1261/RNA.1997610.
92. Vinayak, M., Pathak, C., (2009). Queuosine modification of tRNA: its divergent role in cellular machinery. *Biosci. Rep.* **30**, 135–148. https://doi.org/10.1042/BSR20090057.
93. Fergus, C., Barnes, D., Alqasem, M.A., Kelly, V.P., (2015). The queuine micronutrient: charting a course from microbe to man. *Nutrients* **7**, 2897. https://doi.org/10.3390/NU7042897.
94. Alqasem, M.A., Fergus, C., Southern, J.M., Connon, S.J., Kelly, V.P., (2020). The eukaryotic tRNA-guanine transglycosylase enzyme inserts queuine into tRNA via a sequential bi-bi mechanism. *Chem. Commun. (Camb.)* **56**, 3915–3918. https://doi.org/10.1039/C9CC09887A.
95. Sievers, K., Neumann, P., Sušac, L., Da Vela, S., Graewert, M., Trowitzsch, S., Svergun, D., Tampé, R., Ficner, R., (2024). Structural and functional insights into tRNA recognition by human tRNA guanine transglycosylase. *Structure* **32**, 316–327.e5. https://doi.org/10.1016/J.STR.2023.12.006.
96. Suzuki, T., Ogizawa, A., Ishiguro, K., Nagao, A., (2024). Biogenesis and roles of tRNA queuosine modification and its glycosylated derivatives in human health and diseases. *Cell Chem. Biol.*. https://doi.org/10.1016/J.CHEMBIOL.2024.11.004.
97. Rashad, S., (2025). Queuosine tRNA modification: connecting the microbiome to the translatome. *Bioessays* **47**, e202400213. https://doi.org/10.1002/bies.202400213.
98. Rintala-Dempsey, A.C., Kothe, U., (2017). Eukaryotic stand-alone pseudouridine synthases – RNA modifying enzymes and emerging regulators of gene expression?. *RNA Biol.* **14**, 1185–1196. https://doi.org/10.1080/15476286.2016.1276150.
99. Shaheen, R., Han, L., Faqeih, E., Ewida, N., Alobeid, E., Phizicky, E.M., Alkuraya, F.S., (2016). A homozygous truncating mutation in PUS3 expands the role of tRNA modification in normal cognition. *Hum. Genet.* **135**, 707–713. https://doi.org/10.1007/s00439-016-1665-7.
100. Lin, T.-Y., Kleemann, L., Jeżowski, J., Dobosz, D., Rawski, M., Indyka, P., Ważny, G., Mehta, R., Chramiec-Głąbik, A., Koziej, Ł., Ranff, T., Fufezan, C., Wawro, M., Kochan, J., Bereta, J., Leidel, S.A., Glatt, S., (2024). The molecular basis of tRNA selectivity by human pseudouridine synthase 3. *Mol. Cell* **84**, 2472–2489.e8. https://doi.org/10.1016/j.molcel.2024.06.013.
101. De Paiva, A.R.B., Lynch, D.S., Melo, U.S., Lucato, L.T., Freua, F., De Assis, B.D.R., Barcelos, I., Listik, C., De Castro Dos, D., Santos, L.I., MacEdo-Souza, H., Houlden, F.K., (2019). PUS3 mutations are associated with intellectual disability, leukoencephalopathy, and nephropathy. *Neurol. Genet* **5** https://doi.org/10.1212/NXG.0000000000000306.
102. Lin, T.Y., Smigiel, R., Kuzniewska, B., Chmielewska, J.J., Kosińska, J., Biela, M., Biela, A., Kościelniak, A., Dobosz, D., Laczmanska, I., Chramiec-Głąbik, A., Jeżowski, J., Nowak, J., Gos, M., Rzonca-Niewczas, S., Dziembowska, M., Ploski, R., Glatt, S., (2022). Destabilization of mutated human PUS3 protein causes intellectual disability. *Hum. Mutat.*, 2063–2078. https://doi.org/10.1002/humu.24471.
103. Vilardo, E., Nachbagauer, C., Buzet, A., Taschner, A., Holzmann, J., Rossmanith, W., (2012). A subcomplex of human mitochondrial RNase P is a bifunctional methyltransferase–extensive moonlighting in mitochondrial tRNA biogenesis. *Nucleic Acids Res.* **40**, 11583–11593. https://doi.org/10.1093/nar/gks910.
104. Shao, Z., Yan, W., Peng, J., Zuo, X., Zou, Y., Li, F., Gong, D., Ma, R., Wu, J., Shi, Y., Zhang, Z., Teng, M., Li, X., Gong, Q., (2014). Crystal structure of tRNA m1G9 methyltransferase Trm10: insight into the catalytic mechanism and recognition of tRNA substrate. *Nucleic Acids Res.* **42**, 509–525. https://doi.org/10.1093/NAR/GKT869.
105. Vilardo, E., Amman, F., Toth, U., Kotter, A., Helm, M., Rossmanith, W., (2020). Functional characterization of the human tRNA methyltransferases TRMT10A and TRMT10B. *Nucleic Acids Res.* **48**, 6157–6169. https://doi.org/10.1093/nar/gkaa353.
106. Howell, N.W., Jora, M., Jepson, B.F., Limbach, P.A., Jackman, J.E., (2019). Distinct substrate specificities of the human tRNA methyltransferases TRMT10A and TRMT10B. *RNA* **25**, 1366–1376. https://doi.org/10.1261/rna.072090.119.
107. Reinhard, L., Sridhara, S., Hällberg, B.M., (2017). The MRPP1/MRPP2 complex is a tRNA-maturation platform in human mitochondria. *Nucleic Acids Res.* **45**, 12469. https://doi.org/10.1093/NAR/GKX902.
108. Meynier, V., Hardwick, S.W., Catala, M., Roske, J.J., Oerum, S., Chirgadze, D.Y., Barraud, P., Yue, W.W., Luisi, B.F., Tisné, C., (2024). Structural basis for human mitochondrial tRNA maturation. *Nature Commun.* **15** https://doi.org/10.1038/s41467-024-49132-0.
109. Valentín Gesé, G., Hällberg, B.M., (2024). Structural basis of 3′-tRNA maturation by the human mitochondrial RNase Z complex. *EMBO J.* **43**, 6573–6590. https://doi.org/10.1038/s44318-024-00297-w.
110. Bhatta, A., Dienemann, C., Cramer, P., Hillen, H.S., (2021). Structural basis of RNA processing by human mitochondrial RNase P. *Nature Struct. Mol. Biol.* **28**, 713–723. https://doi.org/10.1038/S41594-021-00637-Y.
111. Augustin, M.A., Reichert, A.S., Betat, H., Huber, R., Mörl, M., Steegborn, C., (2003). Crystal structure of the human CCA-adding enzyme: insights into template-independent polymerization. *J. Mol. Biol.* **328**, 985–994. https://doi.org/10.1016/S0022-2836(03)00381-4.
112. Helm, M., Brulé, H., Degoul, F., Cepanec, C., Leroux, J. P., Giegé, R., Florentz, C., (1998). The presence of modified nucleotides is required for cloverleaf folding of a human mitochondrial tRNA. *Nucleic Acids Res.* **26**, 1636–1643. https://doi.org/10.1093/nar/26.7.1636.
113. Helm, M., Giegé, R., Florentz, C., (1999). A Watson-Crick base-pair-disrupting methyl group (m1A9) is sufficient for cloverleaf folding of human mitochondrial tRNALys. *Biochemistry* **38**, 13338–13346. https://doi.org/10.1021/bi991061g.
114. Bhatta, A., Kuhle, B., Yu, R.D., Spanaus, L., Ditter, K., Bohnsack, K.E., Hillen, H.S., (2025). Molecular basis of human nuclear and mitochondrial tRNA 3′ processing. *Nature Struct. Mol. Biol.*. https://doi.org/10.1038/S41594-024-01445-W.
115. Oerum, S., Roovers, M., Rambo, R.P., Kopec, J., Bailey, H.J., Fitzpatrick, F., Newman, J.A., Newman, W.G., Amberger, A., Zschocke, J., Droogmans, L., Oppermann, U., Yue, W.W., (2018). Structural insight into the human mitochondrial tRNA purine N1-methyltransferase and ribonuclease P complexes. *J.*

Biol. Chem. **293**, 12862–12876. https://doi.org/10.1074/JBC.RA117.001286.
116. Sikarwar, J., Meynier, V., Tisné, C., (2025). Advances in human Pre-tRNA maturation: TRMT10C and ELAC2 in focus. *J. Mol. Biol.*168989. https://doi.org/10.1016/j.jmb.2025.168989.
117. Abbassi, N.E.H., Jaciuk, M., Scherf, D., Böhnert, P., Rau, A., Hammermeister, A., Rawski, M., Indyka, P., Wazny, G., Chramiec-Głąbik, A., Dobosz, D., Skupien-Rabian, B., Jankowska, U., Rappsilber, J., Schaffrath, R., Lin, T.Y., Glatt, S., (2024). Cryo-EM structures of the human Elongator complex at work. *Nature Commun.* **15** https://doi.org/10.1038/S41467-024-48251-Y.
118. Dauden, M.I., Kosinski, J., Kolaj-Robin, O., Desfosses, A., Ori, A., Faux, C., Hoffmann, N.A., Onuma, O.F., Breunig, K.D., Beck, M., Sachse, C., Seraphin, B., Glatt, S., Muller, C.W., (2017). Architecture of the yeast Elongator complex. *EMBO Rep.* **18**, 264–279. https://doi.org/10.15252/embr.201643353.
119. Glatt, S., Letoquart, J., Faux, C., Taylor, N.M., Seraphin, B., Muller, C.W., (2012). The Elongator subcomplex Elp456 is a hexameric RecA-like ATPase. *Nature Struct. Mol. Biol.* **19**, 314–320. https://doi.org/10.1038/nsmb.2234.
120. Jaciuk, M., Scherf, D., Kaszuba, K., Gaik, M., Rau, A., Kościelniak, A., Krutyhołowa, R., Rawski, M., Indyka, P., Graziadei, A., Chramiec-Głąbik, A., Biela, A., Dobosz, D., Lin, T.-Y., Abbassi, N.-E.-H., Hammermeister, A., Rappsilber, J., Kosinski, J., Schaffrath, R., Glatt, S., (2023). Cryo-EM structure of the fully assembled Elongator complex. *Nucleic Acids Res.*. https://doi.org/10.1093/NAR/GKAC1232.
121. Hawer, H., Hammermeister, A., Ravichandran, K.E., Glatt, S., Schaffrath, R., Klassen, R., (2018). Roles of Elongator dependent tRNA modification pathways in neurodegeneration and cancer. *Genes (Basel)* **10**, 19. https://doi.org/10.3390/genes10010019.
122. Selvadurai, K., Wang, P., Seimetz, J., Huang, R.H., (2014). Archaeal Elp3 catalyzes tRNA wobble uridine modification at C5 via a radical mechanism. *Nature Chem. Biol.* **10**, 810–812. https://doi.org/10.1038/nchembio.1610.
123. Gaik, M., Kojic, M., Wainwright, B.J., Glatt, S., (2022). Elongator and the role of its subcomplexes in human diseases. *EMBO Mol. Med.*. https://doi.org/10.15252/EMMM.202216418.
124. Haag, S., Warda, A.S., Kretschmer, J., Günnigmann, M. A., Höbartner, C., Bohnsack, M.T., (2015). NSUN6 is a human RNA methyltransferase that catalyzes formation of m5C72 in specific tRNAs. *RNA* **21**, 1532–1543. https://doi.org/10.1261/rna.051524.115.
125. Liu, R.-J., Long, T., Li, J., Li, H., Wang, E.-D., (2017). Structural basis for substrate binding and catalytic mechanism of a human RNA:m 5 C methyltransferase NSun6. *Nucleic Acids Res.* **45**, 6684–6697. https://doi.org/10.1093/nar/gkx473.
126. Long, T., Li, J., Li, H., Zhou, M., Zhou, X.-L., Liu, R.-J., Wang, E.-D., (2016). Sequence-specific and shape-selective RNA recognition by the human RNA 5-methylcytosine methyltransferase NSun6. *J. Biol. Chem.* **291**, 24293–24303. https://doi.org/10.1074/jbc.M116.742569.
127. Li, C., Wang, S., Xing, Z., Lin, A., Liang, K., Song, J., Hu, Q., Yao, J., Chen, Z., Park, P.K., Hawke, D.H., Zhou, J., Zhou, Y., Zhang, S., Liang, H., Hung, M.-C., Gallick, G.E., Han, L., Lin, C., Yang, L., (2017). A ROR1-HER3-lncRNA signalling axis modulates the Hippo-YAP pathway to regulate bone metastasis. *Nature Cell Biol.* **19**, 106–119. https://doi.org/10.1038/ncb3464.
128. Finer-Moore, J., Czudnochowski, N., O'Connell, J.D., Wang, A.L., Stroud, R.M., (2015). Crystal structure of the human tRNA m1A58 methyltransferase-tRNA3Lys complex: refolding of substrate tRNA allows access to the methylation target. *J. Mol. Biol.* **427**, 3862–3876. https://doi.org/10.1016/J.JMB.2015.10.005.
129. Ozanick, S., Krecic, A., Andersland, J., Anderson, J.T., (2005). The bipartite structure of the tRNA m1A58 methyltransferase from *S. cerevisiae* is conserved in humans. *RNA* **11**, 1281–1290. https://doi.org/10.1261/RNA.5040605.
130. Su, Z., Monshaugen, I., Wilson, B., Wang, F., Klungland, A., Ougland, R., Dutta, A., (2022). TRMT6/61A-dependent base methylation of tRNA-derived fragments regulates gene-silencing activity and the unfolded protein response in bladder cancer. *Nature Commun.* **13** https://doi.org/10.1038/S41467-022-29790-8.
131. Wang, Y., Wang, J., Li, X., Xiong, X., Wang, J., Zhou, Z., Zhu, X., Gu, Y., Dominissini, D., He, L., Tian, Y., Yi, C., Fan, Z., (2021). N1-methyladenosine methylation in tRNA drives liver tumourigenesis by regulating cholesterol metabolism. *Nature Commun.* **12** https://doi.org/10.1038/S41467-021-26718-6.
132. Alexandrov, A., Martzen, M.R., Phizicky, E.M., (2002). Two proteins that form a complex are required for 7-methylguanosine modification of yeast tRNA. *RNA* **8**, 1253–1266. https://doi.org/10.1017/s1355838202024019.
133. Ruiz-Arroyo, V.M., Raj, R., Babu, K., Onolbaatar, O., Roberts, P.H., Nam, Y., (2023). Structures and mechanisms of tRNA methylation by METTL1–WDR4. *Nature* **613**, 383–390. https://doi.org/10.1038/s41586-022-05565-5.
134. Li, J., Wang, L., Hahn, Q., Nowak, R.P., Viennet, T., Orellana, E.A., Roy Burman, S.S., Yue, H., Hunkeler, M., Fontana, P., Wu, H., Arthanari, H., Fischer, E.S., Gregory, R.I., (2023). Structural basis of regulated m7G tRNA modification by METTL1–WDR4. *Nature* **613**, 391–397. https://doi.org/10.1038/s41586-022-05566-4.
135. Cartlidge, R.A., Knebel, A., Peggie, M., Alexandrov, A., Phizicky, E.M., Cohen, P., (2005). The tRNA methylase METTL1 is phosphorylated and inactivated by PKB and RSK in vitro and in cells. *EMBO J.* **24**, 1696–1705. https://doi.org/10.1038/SJ.EMBOJ.7600648.
136. Xu, L., Liu, X., Sheng, N., Oo, K.S., Liang, J., Chionh, Y. H., Xu, J., Ye, F., Gao, Y.G., Dedon, P.C., Fu, X.Y., (2017). Three distinct 3-methylcytidine (m3C) methyltransferases modify tRNA and mRNA in mice and humans. *J. Biol. Chem.* **292**, 14695–14703. https://doi.org/10.1074/JBC.M117.798298.
137. Mao, X.L., Li, Z.H., Huang, M.H., Wang, J.T., Zhou, J.B., Li, Q.R., Xu, H., Wang, X.J., Zhou, X.L., (2021). Mutually exclusive substrate selection strategy by human m3C RNA transferases METTL2A and METTL6. *Nucleic Acids Res.* **49**, 8309–8323. https://doi.org/10.1093/NAR/GKAB603.
138. Throll, P., Dolce, L.G., Rico-Lastres, P., Arnold, K., Tengo, L., Basu, S., Kaiser, S., Schneider, R., Kowalinski, E., (2024). Structural basis of tRNA

recognition by the m3C RNA methyltransferase METTL6 in complex with SerRS seryl-tRNA synthetase. *Nature Struct. Mol. Biol.* **31**, 1614–1624. https://doi.org/10.1038/s41594-024-01341-3.
139. Lentini, J.M., Alsaif, H.S., Faqeih, E., Alkuraya, F.S., Fu, D., (2020). DALRD3 encodes a protein mutated in epileptic encephalopathy that targets arginine tRNAs for 3-methylcytosine modification. *Nature Commun.* **11**, 2510. https://doi.org/10.1038/s41467-020-16321-6.
140. Li, S., Zhou, H., Liao, S., Wang, X., Zhu, Z., Zhang, J., Xu, C., (2022). Structural basis for METTL6-mediated m3C RNA methylation. *Biochem. Biophys. Res. Commun.* **589**, 159–164. https://doi.org/10.1016/J.BBRC.2021.12.013.
141. Ignatova, V.V., Kaiser, S., Ho, J.S.Y., Bing, X., Stolz, P., Tan, Y.X., Lee, C.L., Gay, F.P.H., Lastres, P.R., Gerlini, R., Rathkolb, B., Aguilar-Pimentel, A., Sanz-Moreno, A., Klein-Rodewald, T., Calzada-Wack, J., Ibragimov, E., Valenta, M., Lukauskas, S., Pavesi, A., Marschall, S., Leuchtenberger, S., Fuchs, H., Gailus-Durner, V., De Angelis, M.H., Bultmann, S., Rando, O.J., Guccione, E., Kellner, S.M., Schneider, R., (2020). METTL6 is a tRNA m3C methyltransferase that regulates pluripotency and tumor cell growth. *Sci Adv 6*eaaz4551. https://doi.org/10.1126/SCIADV.AAZ4551.
142. Bolatkan, A., Asada, K., Kaneko, S., Suvarna, K., Ikawa, N., Machino, H., Komatsu, M., Shiina, S., Hamamoto, R., (2022). Downregulation of METTL6 mitigates cell progression, migration, invasion and adhesion in hepatocellular carcinoma by inhibiting cell adhesion molecules. *Int. J. Oncol.* **60** https://doi.org/10.3892/IJO.2021.5294.
143. Jumper, J., Evans, R., Pritzel, A., Green, T., Figurnov, M., Ronneberger, O., Tunyasuvunakool, K., Bates, R., Žídek, A., Potapenko, A., Bridgland, A., Meyer, C., Kohl, S.A.A., Ballard, A.J., Cowie, A., Romera-Paredes, B., Nikolov, S., Jain, R., Adler, J., Back, T., Petersen, S., Reiman, D., Clancy, E., Zielinski, M., Steinegger, M., Pacholska, M., Berghammer, T., Bodenstein, S., Silver, D., Vinyals, O., Senior, A.W., Kavukcuoglu, K., Kohli, P., Hassabis, D., (2021). Highly accurate protein structure prediction with AlphaFold. *Nature* **596** https://doi.org/10.1038/s41586-021-03819-2.
144. Abramson, J., Adler, J., Dunger, J., Evans, R., Green, T., Pritzel, A., Ronneberger, O., Willmore, L., Ballard, A.J., Bambrick, J., Bodenstein, S.W., Evans, D.A., Hung, C.-C., O'Neill, M., Reiman, D., Tunyasuvunakool, K., Wu, Z., Žemgulytė, A., Arvaniti, E., Beattie, C., Bertolli, O., Bridgland, A., Cherepanov, A., Congreve, M., Cowen-Rivers, A.I., Cowie, A., Figurnov, M., Fuchs, F.B., Gladman, H., Jain, R., Khan, Y.A., Low, C.M.R., Perlin, K., Potapenko, A., Savy, P., Singh, S., Stecula, A., Thillaisundaram, A., Tong, C., Yakneen, S., Zhong, E.D., Zielinski, M., Žídek, A., Bapst, V., Kohli, P., Jaderberg, M., Hassabis, D., Jumper, J.M., (2024). Accurate structure prediction of biomolecular interactions with AlphaFold 3. *Nature* **630**, 493–500. https://doi.org/10.1038/s41586-024-07487-w.
145. Lombard, M., Reed, C.J., Pecqueur, L., Faivre, B., Toubdji, S., Sudol, C., Brégeon, D., de Crécy-Lagard, V., Hamdane, D., (2022). Evolutionary diversity of Dus2 enzymes reveals novel structural and functional features among members of the RNA dihydrouridine synthases family. *Biomolecules* **12** https://doi.org/10.3390/biom12121760.
146. Lin, T.Y., Mehta, R., Glatt, S., (2021). Pseudouridines in RNAs: switching atoms means shifting paradigms. *FEBS Lett.* **595**, 2310–2322. https://doi.org/10.1002/1873-3468.14188.
147. Zhou, C., Huang, R.H., (2008). Crystallographic snapshots of eukaryotic dimethylallyltransferase acting on tRNA: insight into tRNA recognition and reaction mechanism. *PNAS* **105**, 16142–16147. https://doi.org/10.1073/pnas.0805680105.
148. Cheng, J., Baßler, J., Fischer, P., Lau, B., Kellner, N., Kunze, R., Griesel, S., Kallas, M., Berninghausen, O., Strauss, D., Beckmann, R., Hurt, E., (2019). Thermophile 90S pre-ribosome structures reveal the reverse order of Co-transcriptional 18S rRNA subdomain integration. *Mol. Cell* **75**, 1256–1269.e7. https://doi.org/10.1016/j.molcel.2019.06.032.
149. Takakura, M., Ishiguro, K., Akichika, S., Miyauchi, K., Suzuki, T., (2019). Biogenesis and functions of aminocarboxypropyluridine in tRNA. *Nature Commun.* **10** https://doi.org/10.1038/S41467-019-13525-3.
150. Perche-Letuvée, P., Molle, T., Forouhar, F., Mulliez, E., Atta, M., (2014). Wybutosine biosynthesis: structural and mechanistic overview. *RNA Biol.* **11**, 1508–1518. https://doi.org/10.4161/15476286.2014.992271.
151. Erie De Crécy, V., Crécy-Lagard, C., Boccaletto, P., Mangleburg, C.G., Sharma, P., Lowe, T.M., Leidel, S.A., Bujnicki, J.M., (2019). SURVEY AND SUMMARY Matching tRNA modifications in humans to their known and predicted enzymes. *Nucleic Acids Res.* **47**, 2143–2159. https://doi.org/10.1093/nar/gkz011.
152. Abbassi, N.E.H., Biela, A., Glatt, S., Lin, T.Y., (2020). How elongator acetylates trna bases. *Int. J. Mol. Sci.* **21**, 1–13. https://doi.org/10.3390/ijms21218209.
153. Leidel, S., Pedrioli, P.G.A., Bucher, T., Brost, R., Costanzo, M., Schmidt, A., Aebersold, R., Boone, C., Hofmann, K., Peter, M., (2009). Ubiquitin-related modifier Urm1 acts as a sulphur carrier in thiolation of eukaryotic transfer RNA. *Nature* **458**, 228–232. https://doi.org/10.1038/nature07643.
154. Noma, A., Sakaguchi, Y., Suzuki, T., (2009). Mechanistic characterization of the sulfur-relay system for eukaryotic 2-thiouridine biogenesis at tRNA wobble positions. *Nucleic Acids Res.* **37**, 1335–1352. https://doi.org/10.1093/nar/gkn1023.
155. Huang, B.O., Lu, J., Bystro, A.S., (2008). A genome-wide screen identifies genes required for formation of the wobble nucleoside in *Saccharomyces cerevisiae*. *RNA* **14**, 2183–2194. https://doi.org/10.1261/rna.1184108.2.
156. Marelja, Z., Stöcklein, W., Nimtz, M., Leimkühler, S., (2008). A novel role for human Nfs1 in the cytoplasm: Nfs1 acts as a sulfur donor for MOCS3, a protein involved in molybdenum cofactor biosynthesis. *J. Biol. Chem.* **283**, 25178–25185. https://doi.org/10.1074/jbc.M804064200.
157. Dewez, M., Bauer, F., Dieu, M., Raes, M., Vandenhaute, J., Hermand, D., (2008). The conserved Wobble uridine tRNA thiolase Ctu1-Ctu2 is required to maintain genome integrity. *PNAS* **105**, 5459–5464. https://doi.org/10.1073/pnas.0709404105.
158. Shigi, N., (2018). Recent advances in our understanding of the biosynthesis of sulfur modifications in tRNAs. *Front. Microbiol.* **9**, 1–9. https://doi.org/10.3389/fmicb.2018.02679.
159. Arragain, S., Bimai, O., Legrand, P., Caillat, S., Ravanat, J.-L., Touati, N., Binet, L., Atta, M., Fontecave, M.,

Golinelli-Pimpaneau, (2017). Nonredox thiolation in tRNA occurring via sulfur activation by a [4Fe-4S] cluster. *PNAS* **114**, 7355–7360. https://doi.org/10.1073/pnas.1700902114.

160. Chen, M., Asai, S.I., Narai, S., Nambu, S., Omura, N., Sakaguchi, Y., Suzuki, T., Ikeda-Saito, M., Watanabe, K., Yao, M., Shigi, N., Tanaka, Y., (2017). Biochemical and structural characterization of oxygen-sensitive 2-thiouridine synthesis catalyzed by an iron-sulfur protein TtuA. *PNAS*. https://doi.org/10.1073/pnas.1615585114.
161. Chen, M., Narai, S., Omura, N., Shigi, N., Chimnaronk, S., Tanaka, Y., Yao, M., (2016). Crystallographic study of the 2-thioribothymidine-synthetic complex TtuA-TtuB from *Thermus thermophilus*. *Acta Crystallogr. F Struct. Biol. Commun.* **72**, 777–781. https://doi.org/10.1107/S2053230X16014242.
162. Chen, M., Ishizaka, M., Narai, S., Horitani, M., Shigi, N., Yao, M., Tanaka, Y., (2020). The [4Fe-4S] cluster of sulfurtransferase TtuA desulfurizes TtuB during tRNA modification in *Thermus thermophilus*. *Commun. Biol.* **3** https://doi.org/10.1038/s42003-020-0895-3.
163. Ishizaka, M., Chen, M., Narai, S., Tanaka, Y., Ose, T., Horitani, M., Yao, M., (2023). Quick and spontaneous transformation between [3Fe–4S] and [4Fe–4S] iron–sulfur clusters in the tRNA-thiolation enzyme TtuA. *Int. J. Mol. Sci.* **24** https://doi.org/10.3390/ijms24010833.
164. Shaheen, R., Patel, N., Shamseldin, H., Alzahrani, F., Al-Yamany, R., Almoisheer, A., Ewida, N., Anazi, S., Alnemer, M., Elsheikh, M., Alfaleh, K., Alshammari, M., Alhashem, A., Alangari, A.A., Salih, M.A., Kircher, M., Daza, R.M., Ibrahim, N., Wakil, S.M., Alaqeel, A., Altowaijri, I., Shendure, J., Al-Habib, A., Faqieh, E., Alkuraya, F.S., (2016). Accelerating matchmaking of novel dysmorphology syndromes through clinical and genomic characterization of a large cohort. *Genet. Med.* **18**, 686–695. https://doi.org/10.1038/gim.2015.147.
165. Shaheen, R., Al-Salam, Z., El-Hattab, A.W., Alkuraya, F. S., (2016). The syndrome dysmorphic facies, renal agenesis, ambiguous genitalia, microcephaly, polydactyly and lissencephaly (DREAM-PL): report of two additional patients. *Am. J. Med. Genet. A* **170**, 3222–3226. https://doi.org/10.1002/ajmg.a.37877.
166. Shaheen, R., Mark, P., Prevost, C.T., AlKindi, A., Alhag, A., Estwani, F., Al-Sheddi, T., Alobeid, E., Alenazi, M.M., Ewida, N., Ibrahim, N., Hashem, M., Abdulwahab, F., Bryant, E.M., Spinelli, E., Millichap, J., Barnett, S.S., Kearney, H.M., Accogli, A., Scala, M., Capra, V., Nigro, V., Fu, D., Alkuraya, F.S., (2019). Biallelic variants in *CTU2* cause DREAM-PL syndrome and impair thiolation of tRNA wobble U34. *Hum. Mutat.* **40**, 2108–2120. https://doi.org/10.1002/humu.23870.
167. Wan, L.C.K., Maisonneuve, P., Szilard, R.K., Lambert, J.-P., Ng, T.F., Manczyk, N., Huang, H., Laister, R., Caudy, A.A., Gingras, A.-C., Durocher, D., Sicheri, F., (2017). Proteomic analysis of the human KEOPS complex identifies C14ORF142 as a core subunit homologous to yeast Gon7. *Nucleic Acids Res.* **45**, 805–817. https://doi.org/10.1093/nar/gkw1181.
168. Mao, D.Y.L., Neculai, D., Downey, M., Orlicky, S., Haffani, Y.Z., Ceccarelli, D.F., Ho, J.S.L., Szilard, R.K., Zhang, W., Ho, C.S., Wan, L., Fares, C., Rumpel, S., Kurinov, I., Arrowsmith, C.H., Durocher, D., Sicheri, F., (2008). Atomic structure of the KEOPS complex: an ancient protein kinase-containing molecular machine. *Mol. Cell* **32**, 259–275. https://doi.org/10.1016/J.MOLCEL.2008.10.002.
169. Li, J., Ma, X., Banerjee, S., Chen, H., Ma, W., Bode, A.M., Dong, Z., (2021). Crystal structure of the human PRPK-TPRKB complex. *Commun. Biol.* **4**, 167. https://doi.org/10.1038/s42003-021-01683-4.
170. Perrochia, L., Crozat, E., Hecker, A., Zhang, W., Bareille, J., Collinet, B., Van Tilbeurgh, H., Forterre, P., Basta, T., (2012). In vitro biosynthesis of a universal t6A tRNA modification in Archaea and Eukarya. *Nucleic Acids Res.* **41**, 1953. https://doi.org/10.1093/NAR/GKS1287.
171. Srinivasan, M., Mehta, P., Yu, Y., Prugar, E., Koonin, E. V., Karzai, A.W., Sternglanz, R., (2011). The highly conserved KEOPS/EKC complex is essential for a universal tRNA modification, t6A. *EMBO J* **30**, 873–881. https://doi.org/10.1038/EMBOJ.2010.343.
172. Han, L., Phizicky, E.M., (2018). A rationale for tRNA modification circuits in the anticodon loop. *RNA*. https://doi.org/10.1261/rna.067736.118.
173. Il Kang, B., Miyauchi, K., Matuszewski, M., D'Almeida, G. S., Rubio, M.A.T., Alfonzo, J.D., Inoue, K., Sakaguchi, Y., Suzuki, T., Sochacka, E., Suzuki, T., (2017). Identification of 2-methylthio cyclic N6-threonylcarbamoyladenosine (ms2ct6A) as a novel RNA modification at position 37 of tRNAs. *Nucleic Acids Res.* **45**, 2124–2136. https://doi.org/10.1093/NAR/GKW1120.
174. Ona Chuquimarca, S.M., Beenstock, J., Daou, S., Porat, J., Keszei, A.F.A., Yin, J.Z., Beschauner, T., Bayfield, M. A., Mazhab-Jafari, M.T., Sicheri, F., (2024). Structures of KEOPS bound to tRNA reveal functional roles of the kinase Bud32. *Nature Commun.* **15** https://doi.org/10.1038/S41467-024-54787-W.
175. Zheng, X., Su, C., Duan, L., Jin, M., Sun, Y., Zhu, L., Zhang, W., (2024). Molecular basis of A. thaliana KEOPS complex in biosynthesizing tRNA t6A. *Nucleic Acids Res.* **52**, 4523–4540. https://doi.org/10.1093/nar/gkae179.
176. Arrondel, C., Missoury, S., Snoek, R., Patat, J., Menara, G., Collinet, B., Liger, D., Durand, D., Gribouval, O., Boyer, O., Buscara, L., Martin, G., Machuca, E., Nevo, F., Lescop, E., Braun, D.A., Boschat, A.C., Sanquer, S., Guerrera, I.C., Revy, P., Parisot, M., Masson, C., Boddaert, N., Charbit, M., Decramer, S., Novo, R., Macher, M.A., Ranchin, B., Bacchetta, J., Laurent, A., Collardeau-Frachon, S., van Eerde, A.M., Hildebrandt, F., Magen, D., Antignac, C., van Tilbeurgh, H., Mollet, G., (2019). Defects in t6A tRNA modification due to GON7 and YRDC mutations lead to Galloway-Mowat syndrome. *Nature Commun.* **10** https://doi.org/10.1038/S41467-019-11951-X.
177. Weissmann, F., Peters, J., (2018). Expressing multi-subunit complexes using biGBac. *Methods Mol. Biol.* **1764**, 329–343.
178. Miao, Z., Westhof, E., Structure, R.N.A., (2017). Advances and assessment of 3D structure prediction. *Annu. Rev. Biophys.* **46**, 483–503. https://doi.org/10.1146/annurev-biophys-070816-034125.